

Report No. UT-10.20

ASSESSING CORROSION OF MSE WALL REINFORCEMENT

Prepared For:

Utah Department of Transportation
Research Division

Submitted By:

Brigham Young University
Dept. of Civil & Environmental Engineering

Authored By:

Travis M. Gerber and Daniel A. Billings

September 2010

THIS PAGE LEFT INTENTIONALLY BLANK

DISCLAIMER:

“The authors alone are responsible for the preparation and accuracy of the information, data, analysis, discussions, recommendations, and conclusions presented herein. The contents do not necessarily reflect the views, opinions, endorsements, or policies of the Utah Department of Transportation or the U.S. Department of Transportation. The Utah Department of Transportation makes no representation or warranty of any kind, and assumes no liability therefore.”

THIS PAGE LEFT INTENTIONALLY BLANK

Technical Report Documentation Page

1. Report No. UT- 10.20		2. Government Accession No.		3. Recipient's Catalog No.	
4. Title and Subtitle ASSESSING CORROSION OF MSE WALL REINFORCEMENT				5. Report Date September 2010	
				6. Performing Organization Code	
7. Author Travis M. Gerber and Daniel A. Billings				8. Performing Organization Report No. BYU Report No. CEG 2010-01	
9. Performing Organization Name and Address Department of Civil & Environmental Engineering Brigham Young University 368 CB Provo, UT 84602				10. Work Unit No. 5H06496H	
				11. Contract or Grant No. 10-9262	
12. Sponsoring Agency Name and Address Utah Department of Transportation 4501 South 2700 West Mailing Address: P.O. Box 148410 Salt Lake City, Utah 84114-8410				13. Type of Report & Period Covered FINAL April 2010 to Sept 2010	
				14. Sponsoring Agency Code PIC No. UT09.703	
15. Supplementary Notes Prepared in cooperation with the Utah Department of Transportation					
16. Abstract <p>The primary objective of this study was to extract reinforcement coupons from select MSE walls and document the extent of corrosion. In doing this, a baseline has been established against which coupons extracted in the future can be compared. A secondary objective of this project was to develop and assess techniques for removal of coupons on two-stage MSE walls. Twenty-two wire coupons were extracted from MSE walls that are approximately 11 to 12 years old. Based on field observations, coupon galvanization appeared to be intact but exhibited a variable amount of white oxidation product. In some places the galvanization appeared to have flaked or spalled from the underlying steel, and a minor amount of localized steel corrosion was observed on several of such specimens. Based on laboratory acid-stripping tests, the average thickness of the galvanization on all of the extracted coupons currently exceeds the minimum value specified for the time of installation. Because the initial conditions are unknown, a reliable corrosion rate could not be determined using the direct measurement methods employed in this study. However, the data collected regarding current conditions can be used as baseline information going forward to compute corrosion rates in the future. No readily discernable difference in corrosion conditions as a function of distance away from the wall face was found. There was significance difference in the coupon pullout resistance between one-stage and two-stage MSE walls. The reasons for this behavior and their implications for design and performance should be investigated further.</p>					
17. Key Words Mechanically stabilized earth walls, MSE walls, corrosion		18. Distribution Statement Not restricted. Available through: UDOT Research Division P.O. Box 148410 Salt Lake City, Utah 84114-8410 www.udot.utah.gov		23. Registrant's Seal	
19. Security Classification (of this report) Unclassified	20. Security Classification (of this page) Unclassified	21. No. of Pages 70	22. Price		

THIS PAGE LEFT INTENTIONALLY BLANK

ACKNOWLEDGEMENTS

We the authors wish to recognize David Stevens of UDOT (Utah Department of Transportation) who provided managerial oversight for the project; Grant Gummow and Blaine Leonard of UDOT who helped champion the project; Si Sakhai formerly of UDOT who graciously shared his personal files with the authors; and Rick Chesnut of Terracon and Mathew Francis of URS Corporation for providing access to their companies' I-15 Corridor Reconstruction project files.

THIS PAGE LEFT INTENTIONALLY BLANK

TABLE OF CONTENTS

LIST OF TABLES	xi
LIST OF FIGURES	xiii
EXECUTIVE SUMMARY	1
1.0 INTRODUCTION	3
1.1 General.....	3
1.2 Objective.....	3
2.0 BACKGROUND INFORMATION	5
2.1 MSE Walls.....	5
2.2 Corrosion Process	5
2.3 Corrosion Protection	7
2.4 Corrosion Rates.....	7
2.5 MSE Wall Assessment Practices	11
3.0 COLLECTION OF DATA	15
3.1 Collection of Existing Information	15
3.2 Development of Coupon Extraction Procedure	17
3.3 Coupon Extraction and General Observations.....	21
4.0 ANALYSIS AND INTERPRETATION OF CORROSION DATA.....	25
4.1 Methods of Analysis	25
4.2 Results and Discussion of Results	26
5.0 ANALYSIS AND INTERPRETATION OF PULLOUT RESISTANCE DATA	41
5.1 Methods of Analysis	41
5.2 Results and Discussion of Results	41
6.0 CONCLUSIONS AND RECOMMENDATIONS	49

REFERENCES	51
APPENDIX A.....	55

LIST OF TABLES

Table 1	AASHTO design corrosion rates	8
Table 2	AASHTO electrochemical requirements for MSE wall backfill soils.....	9
Table 3	Summary of UDOT MSE Walls with Extractable Reinforcement Coupons.....	12
Table 4	Steel wire thickness (diameter).....	27
Table 5	Galvanization thickness (in oz/ft ²) by acid stripping (“acid”) and magnetic thickness gauge (“magnet”)	28
Table 6	Galvanization thickness (in mils) by acid stripping (“acid”) and magnetic thickness gauge (“magnet”)	29
Table 7	Amounts of localized steel corrosion.....	33
Table 8	Parameters relating to coupon pullout resistance	42

THIS PAGE LEFT INTENTIONALLY BLANK

LIST OF FIGURES

Figure 1 Schematic of the corrosion process	6
Figure 2 Corrosion versus time for galvanized steel as summarized in draft NCHRP 24-28 report	10
Figure 3 Typical detail for the installation of steel wire coupons for the I-15 Corridor Reconstruction Project	16
Figure 4 Schematic for extraction device	19
Figure 5 Setup of equipment for coupon extraction	20
Figure 6 Alternate setup of equipment for coupon extraction	21
Figure 7 Typical condition of extracted wire coupons	22
Figure 8 Typical view of welded wire mesh through coupon access hole in two-stage MSE wall	23
Figure 9 Segmentation of coupons into specimens for acid stripping test	26
Figure 10 Variation in coupon galvanization thickness.....	31
Figure 11 Photographs detailing damage/loss of galvanization for coupon R-344-1-A-3	34
Figure 12 Photograph detailing corrosion by localized pitting on coupon R-344-1-B-4, specimen A.....	35
Figure 13 Photograph detailing corrosion on coupon R-344-7-A-15, specimen A.....	35
Figure 14 Photograph detailing corrosion of galvanization and steel on coupon R-343-42-A-22, specimen A.....	36
Figure 15 Photograph detailing localized corrosion on coupon R-346-8-A-19, specimen C.....	36
Figure 16 Photograph detailing localized corrosion on coupon R-345-4-A-17, specimen A	37
Figure 17 Damage and subsequent corrosion of coupon R-351-9-B-10 near panel face of two-stage MSE wall	39
Figure 18 Photographs detailing damage and subsequent corrosion near end of coupon R-351-9-B-10.....	39
Figure 19 Coupon pullout resistance normalized by embedded length.....	43
Figure 20 Coupon pullout resistance normalized by embedded length and overburden height..	43

Figure 21 Coupon pullout resistance versus displacement	45
---	----

EXECUTIVE SUMMARY

Mechanically stabilized earth (MSE) walls are now widespread in the Utah Department of Transportation (UDOT)'s retaining wall inventory. Recent inspection work has documented current wall conditions (see Gerber et al. 2008, Bay et al. 2010). Unfortunately, one parameter that could not readily be assessed at the time of that work was the condition of the metallic reinforcement inside many of the MSE walls. Since metallic corrosion can significantly affect the long-term serviceability of MSE walls, it is important to quantify the extent to which detrimental corrosion may or may not be occurring in the reinforcement. The primary objective of this project was to extract buried metallic reinforcement coupons from select MSE walls and document the extent of corrosion. In doing this, a baseline against which coupons extracted in the future can be compared has been established, and data which will help in the assessment of the risk of adverse MSE wall performance is now available. A secondary objective of this project was to develop and assess techniques for removal of coupons on two-stage MSE walls.

Twenty-two wire coupons were extracted from MSE walls that are approximately 11 to 12 years old. Despite extensive searching, no significant information regarding the initial condition of these coupons at the time of their installation was found. Based on field observations, the galvanization on the coupons appeared to be intact but exhibited a variable amount of white oxidation product. In some places the galvanization appeared to have flaked or spalled from the underlying steel. A minor amount of localized steel corrosion was observed on several of such specimens. There was no readily observable evidence of excessive corrosion of the vertical welded wire mesh facing of the two-stage MSE walls.

Based on laboratory acid-stripping tests, the average thickness of the galvanization on all of the extracted coupons currently exceeds the minimum value specified for the time of installation. Because the initial conditions are unknown, a reliable corrosion rate could not be determined using the direct measurement methods employed in this study. However, the data collected regarding current conditions can be used as baseline information going forward to compute corrosion rates in the future. Now that the physical conditions of the coupons are known, consideration should be given to supplementing existing data with linear polarization

resistance (LPR) measurements, a non-destructive, indirect method of determining instantaneous corrosion rates.

Several coupons appeared to have been damaged prior to, or during, installation. Also, the most significant areas of corrosion appeared to be associated with damaged galvanization. Both of these occurrences suggest the need for, and importance of, effective inspection of MSE wall materials prior to installation.

No readily discernable difference in corrosion conditions as a function of distance away from the wall face was found.

There was significant difference in the coupon pullout resistance between one-stage and two-stage MSE walls (with the former being about 4 to 5 times the latter). Current MSE wall design procedures do not suggest that there should be such a difference. The reasons for this behavior and their implications for design and performance should be investigated further.

1.0 INTRODUCTION

1.1 General

Mechanically stabilized earth (MSE) walls are now widespread in the Utah Department of Transportation (UDOT)'s retaining wall inventory. Recent inspection work has documented current wall conditions (see Gerber et al. 2008, Bay et al. 2010). Unfortunately, one parameter that could not readily be assessed was the condition of the metallic reinforcement within the backfill, and in the case of two-stage walls, the welded wire mesh at the wall face. Since corrosion can significantly affect the long-term serviceability of MSE walls, it is important to quantify the extent to which detrimental corrosion may or may not be occurring in the reinforcement. While extractable wire coupons for corrosion testing have been installed in some of UDOT's MSE walls, no wire coupons had been pulled prior to this project and baseline information was unavailable. By determining the current rate of corrosion and/or establishing a baseline now, assessments of MSE wall performance will be much easier and more reliable. This project involved the extraction of MSE wire coupons, documentation of their condition, and estimation of corrosion rates.

1.2 Objective

The primary objective of this project was to extract buried metallic reinforcement coupons from select MSE walls and document the extent of corrosion. By doing this, a baseline against which coupons extracted in the future can be compared has been established, and data which will help in the assessment of the risk of adverse MSE wall performance is now available. A secondary objective of this project was to develop and assess techniques for removal of coupons on two-stage MSE walls.

THIS PAGE LEFT INTENTIONALLY BLANK

2.0 BACKGROUND INFORMATION

2.1 MSE Walls

Mechanically stabilized earth (MSE) is the now generic term for a soil retention wall system that uses reinforcement placed within the backfill (i.e., internal reinforcement) and attached to facing elements, with the fill itself interacting with the reinforcement to resist the lateral loads placed on the wall. MSE walls can be a cost-effective means to retain soil in areas where conventional gravity walls have been used in the past. While many MSE walls have internal reinforcement consisting of inextensible steel meshes or straps, extensible geo-synthetics are also used. Successful performance of MSE walls depends on the integrity of the internal reinforcement. Toward the end of a typical 75- to 100-year service life, there must be enough internal reinforcement remaining after any corrosion (if metallic) or other degradation (if geo-synthetic) to safely resist rupture.

In Utah, two types of MSE walls with inextensible steel reinforcement are commonly used. The first type, called a one-stage MSE wall, is constructed using a concrete panel which retains the backfill and the panel is anchored using welded steel wire mesh or strip reinforcement installed in the backfill. The second, called a two-stage MSE wall, is a variation of the previous type where a welded wire mesh panel (with geosynthetic fabric facing) is used instead of a concrete panel to retain the backfill, and the mesh panel is anchored by similar inextensible reinforcement. This wall type is often used where ground settlements are expected to be relatively large (say in excess of 1 ft for UDOT or 3 ft for some other specifiers) and would be potentially damaging to concrete panels. After the ground finishes settling, permanent concrete facing panels are attached to the mesh panel, thus protecting the wire mesh and geosynthetic fabric and improving the aesthetic appearance of the wall face.

2.2 Corrosion Process

Corrosion of buried steel is a multi-faceted electrochemical process shown schematically in Figure 1 and symbolically in Equations 1a through 1e (after Beavers and Durr 1998). During corrosion, iron atoms in the steel are oxidized in an anodic reaction, thus losing electrons (Equation 1a). Components of the soil (which is composed of minerals, water, air, and possibly organic material) are reduced in a cathodic reaction, thus gaining the previously lost electrons

(Equation 1b through Equation 1d). The current flow in the steel (defined as being from positive to negative charge, opposite the direction of electron flow) is from the cathode to anode, and an equilibrating current flow from anode to cathode is established in the soil, thus forming a corrosion cell. As described by Beavers and Durr (1998), oxygen reduction (Equation 1b) usually controls the rate of corrosion, and this reduction is controlled by the rate of oxygen movement through the soil and water to the steel. Without oxygen present, reduction of water (Equation 1c) occurs; however, this process is very slow. Hydrogen ion reduction (Equation 1d) occurs when the soil is very acidic and can significantly accelerate corrosion. The iron ions produced by oxidation of the steel will react with components in the soil to form corrosion products, including red rust (Equation 1e). Other factors affecting the rate of corrosion are the spatial variability of oxygen and/ or salt concentrations as influenced by soil stratification and water table fluctuations; relative surface area of the anode and the cathode; soil resistivity, and microbiological activity (Beavers and Durr 1998). Stray electrical currents can further exacerbate the corrosion rate. Corrosion is most likely to occur at or just above the water table in disturbed non-uniform soils having low resistivity and/or high soluble salt content.

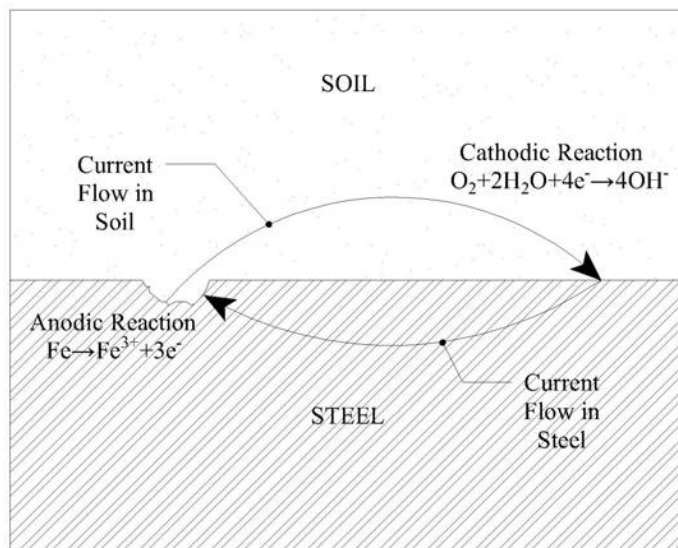
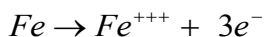


Figure 1 Schematic of the corrosion process



Equation 1a



2.3 Corrosion Protection

To protect against corrosion of steel, a coating of zinc (i.e., galvanization) is frequently used (galvanization is in fact required by the Federal Highway Administration (FHWA) and the American Association of State Highway and Transportation Officials (AASHTO) for internal reinforcement of MSE walls; see Elias and Christopher 1996, Elias et al. 2001, or AASHTO 1996, 2007). The zinc coating initially serves as a mechanical corrosion barrier, preventing moisture and oxygen from coming into contact with the steel. The zinc coating itself experiences corrosion, but at a rate less than that of the steel. Eventually, the coating will become discontinuous and its function as a mechanical barrier will be compromised. However, protection is still afforded to the steel because the exposed steel becomes the cathodic component of the steel-zinc pair, and the tendency for the steel to corrode is counteracted by the flow of electrons from the adjacent, still-corroding zinc (Infinitex Surface Finishing 2005, Elias et al. 2009). Eventually, all of the zinc acting as a sacrificial anode will be consumed and the steel will then experience some characteristic corrosion rate, although the rate may be less than that of initially bare carbon steel due to the presence of the corrosion products resulting from the corroded zinc (Infinitex Surface Finishing 2005, Elias et al. 2009). The amount of steel loss corresponding to the design life is considered as sacrificial and excluded from the gross cross-section in stress design calculations.

2.4 Corrosion Rates

In the U.S., the primary source of information regarding buried metal corrosion rates initially derives from the work of Romanoff (1957) for the National Bureau of Standards (NBS). Subsequently, research more directly applicable to MSE wall backfills was conducted by Terre Armee International (Darbin et al., 1988) and Stuttgart University (Rehm, 1980). The average

loss of steel cross-section due to corrosion is often described using the power law shown in the following equation:

$$x = k \cdot t^n \quad \text{Equation 2}$$

where x is the loss of thickness per side or loss of radius, k and n are empirical constants, and t is the elapsed time with units of years. As summarized by Elias (1990), the “average” loss of zinc for galvanized steel can be described using a coefficient k equal to 0.98 mil (25 μm or micron) and an exponent n equal to 0.65. For bare carbon steel, the average loss of steel can be described using a coefficient k equal to 1.57 mil (40 μm or micron) and an exponent n equal to 0.80. For “maximum” losses (describing localized losses and pitting), the coefficient k is doubled for both materials. This doubling reflects typical findings that the loss of tensile strength due to corrosion is twice that anticipated based strictly on the average loss of cross-section (Jackura et al. 1987, Elias, 1990). Hence, design corrosion rates are usually based on the doubled coefficients.

The accuracy provided by Equation 2 is of course limited to that consistent with an assumed uniform rate of corrosion. A simplified, linearized expression of corrosion rates is provided in FHWA/AASHTO design guidelines. For galvanized steel, these design corrosion rates for maximum losses are shown in Table 1 (after Elias 2000).

Table 1 AASHTO design corrosion rates

Type of Metal and Period of Corrosion	Annual Corrosion Rate per Surface
Zinc, first 2 years	0.59 mil (15 micron)
Zinc, after 2 years (until depletion)	0.16 mil (4 micron)
Carbon steel (after zinc depletion)	0.47 mil (12 micron)

It should be noted that in the case of plate or sheet steel, the total loss in section thickness is double the value otherwise indicated per side. In the case of steel wire or rods, the loss per side or surface corresponds to a radial measurement; hence, the overall increase in diameter due to allowances for galvanization and sacrificial steel is double the value one would calculate “per surface.” The resulting sacrificial total steel thickness (i.e., losses from both sides of a strip or wire) for a 75-year design life based on a minimum initial galvanization thickness of 3.4 mil or

86 micron (which is a typically specified value) is approximately 56 mil or 1.42 mm (Elias et al. 2001).

The rates shown in Table 1 are considered conservative for “non-aggressive” backfill soils, which are defined as soils satisfying the electrochemical requirements shown in Table 2. As clarified by Elias (2000), the previously cited corrosion rates “would be consistent for burial in a wide range of soils, many not meeting the [recommended] restrictive electrochemical requirements for reinforced soil backfills.” Hence, the AASHTO corrosion rates are also applicable for many mildly aggressive soils.

Table 2 AASHTO electrochemical requirements for MSE wall backfill soils

Property	Standard Limit
Resistivity	> 3000 ohm-cm (Ω -cm)
pH	> 5 and < 10
Chlorides	< 100 ppm
Sulfates	< 200 ppm
Organic Content	<= 1%

Updated information regarding corrosion rates are presented by Elias et al. (2009) which incorporates findings of NCHRP [National Cooperative Highway Research Program] Project 24-28, “LRFD Metal Loss and Service-Life Strength Reduction Factors for Metal Reinforced Systems in Geotechnical Applications” (which is currently being finalized as its own project report by Fishman and Withiam (in press)) into an updated version of Elias’ 2001 FHWA design manual, “Corrosion/Degradation of Soil Reinforcements for Mechanically Stabilized Earth Walls and Reinforced Soil Slopes.” In general, existing galvanized metal loss models (including those of NBS and AASHTO presented previously) were found to be conservative. Figure 2 taken from the NCHRP 24-28 draft report shows corrosion (i.e., metal losses) for approximately 404 linear polarization resistance (LPR) measurements (where the measurements are non-destructive and describe the instantaneous corrosion rate) and 50 weight-loss measurements. (Note that many of the data points overlap one another). All of the data comes from soils reportedly satisfying electrochemical requirements similar to AASHTO. On average, longer term (i.e., greater than 2 years) metal loss is about half of what is computed with the AASHTO model, which is consistent

with the design methodology revisions for zinc galvanization recently proposed by Gladstone et al. (2006). For plain steel reinforcement, the average corrosion rate in mildly aggressive soil was founded to be similar to the AASHTO rate. The NCHRP study does provide differentiated corrosion rates based on varying degrees of backfill aggressiveness defined in terms of soil resistivity values. The work of NCHRP 24-28 also determined that “the ratio of maximum metal loss (i.e., loss of tensile strength) to average corrosion rate from LPR measurements range from 1.2 to 4.8 with a mean of 2.4,” as compared to the value of 2 previously discussed by Elias (1990), and notes that there are variations dependent upon the cross-sectional shape of the steel element. This factor appeared to be “inversely proportional to severity of corrosion; and tends to range between 2 and 3 when more severe loss of cross section is observed” (Fishman and Withiam (in press)).

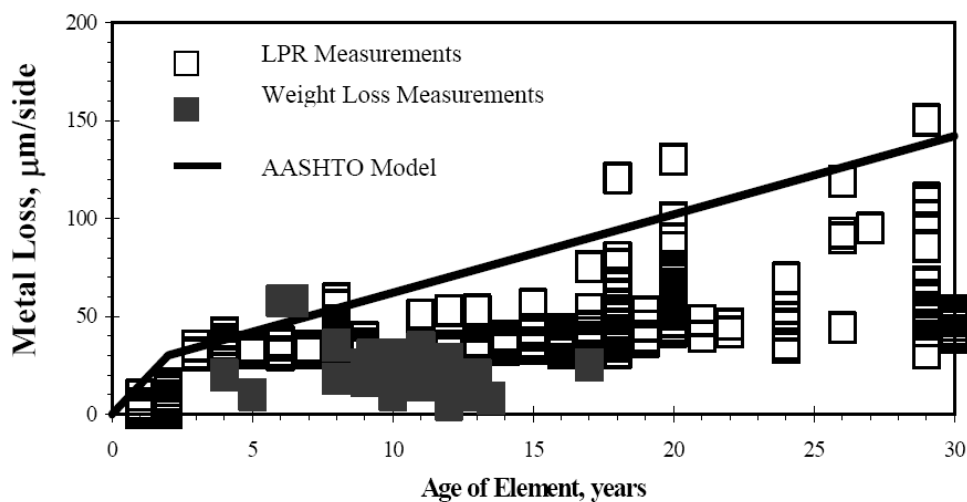


Figure 2 Corrosion versus time for galvanized steel as summarized in draft NCHRP 24-28 report

With respect to spatial location of the reinforcing elements within an MSE wall, the majority of data collected and examined as part of NCHRP 24-28 indicated that “given the limited amount of data and lack of a clear trend, spatial variability is considered to be random” (Fishman and Withiam (in press)). Data from one site in New York, however, did exhibit higher corrosion rates near the wall face compared to deeper within the reinforced fill, and data from several sites in California where multiple inspection elements were spaced 10 feet vertically also suggested that increased corrosion activity may occur near the top of the walls.

2.5 MSE Wall Assessment Practices

As described in the Elias et al. (2009) and Fishman and Withiam (in press), at least nine states (California, Florida, Georgia, Kentucky, Nevada, New York, North Carolina, Ohio, Oregon) assess MSE wall performance and reinforcement corrosion. California appears to be the most active of these states. Motivated by the convergence of several concerns regarding its MSE walls, the Utah Department of Transportation (UDOT) recently sponsored a multi-faceted MSE wall research program. As part of the program, the MSE wall inventory was defined, most of the walls were visited and inspected visually, and a GIS-based database was created. Analytical modeling together with field observations were used to increase UDOT's understanding of adverse performance and causal mechanisms. Using this increased understanding, together with input from a panel of experts (consisting of persons from several transportation agencies, universities, and consulting engineering companies), recommendations for improved design and construction of UDOT MSE walls were developed. Also, since UDOT recognizes that MSE walls are structures with limited life spans (not entirely unlike bridges) which require some level of inspection to assess their condition and assure their serviceability, and because limited funding precludes the implementation of a comprehensive inspection program, a list of walls considered most likely to be problematic was developed. Details of the project are presented in the UDOT project report "An Inspection, Assessment, and Database of UDOT MSE Walls" by Bay et al. (2010), while Gerber et al. (2008) also presents a summary of the project.

An important outcome of the previously described UDOT research effort was the identification of existing MSE wall reinforcement coupon locations. Table 3 summarizes the location, number and arrangement of 216 known UDOT MSE wall reinforcement coupons based on work for the current project as well as information presented in Bay et al. (2010). Coupons, consisting of extractable galvanized wires, were installed in sets of six, sometimes with multiple sets at differing heights. The MSE walls and coupon installations were all constructed during the I-15 Corridor Reconstruction Project through Salt Lake Valley prior to the 2002 Olympics. Wall names come from UDOT's system of structure numbering. The cardinal directions (e.g., NW) listed in the table refer to the corner of the bridge abutment or side of the freeway nearest the coupons. The coupons installed in walls R-342-11 and R-342-13 are buried behind new construction and are no longer accessible.

Table 3 Summary of UDOT MSE Walls with Extractable Reinforcement Coupons

Wall Name	Location	Type	Year Built	No. of Coupons	Comments (coupon height relative to grade at wall base)	Position of Extracted Coupon
R-342-11	10000S and I-15 (SW)	1 Stage	1998	6	Buried behind new MSE wall during expansion of I-15	○ ○ ○ ○ ○ ○
R-342-13	10000S and I-15 (SE)	1 Stage	1998	6	Buried behind new MSE wall during expansion of I-15	○ ○ ○ ○ ○ ○
R-343-07	7200S and I-15 (60ft SW)	1 Stage	1999	12	Extracted R-343-7-A-6 from lower set (5.5ft)	N ● ○ ○ ○ ○ ○ S
R-343-13	7200S and NB I-215 Ramp (100ft NW)	1 Stage	1998	12	Extracted R-343-13-A-8 from lower set (2.8ft)	N ○ ○ ○ ○ ○ ● S
R-343-37	7200S and NB I-215 Ramp (100ft SE)	1 Stage	1998	12	Extracted R-343-37-A-7 from lower set (2.1ft)	S ○ ○ ○ ○ ○ ● N
R-343-42	I-215 WB to I-15 SB Ramp (45ft NW)	1 Stage	1999	6	Extracted R-343-42-A-22	N ● ○ ○ ○ ○ ○ S
R-344-01	5900S and I-15 (250ft SW)	1 Stage	1998	6	Extracted R-344-1-A-3	N ● ○ ○ ○ ○ ○ S
R-344-01	5900S and I-15 (565ft SW)	1 Stage	1998	6	Extracted R-344-1-B-4	N ● ○ ○ ○ ○ ○ S
R-344-02	5900S and I-15 (240ft SE)	1 Stage	1999	6	Extracted R-344-2-A-1	S ○ ○ ○ ○ ○ ● N
R-344-02	5900S and I-15 (490ft SE)	1 Stage	1999	6	Extracted R-344-2-B-2	S ● ○ ○ ○ ○ ○ N
R-344-04	5900S and I-15 (260 NW)	1 Stage	1998	12	Extracted R-344-4-A-5 from lower set (5.1ft)	N ○ ○ ○ ○ ○ ● S
R-344-07	5300S and I-15 (550ft SW)	1 Stage	1998	6	Extracted R-344-7-A-15	N ○ ○ ○ ○ ○ ● S
R-344-11	5300S and I-15 (~200ft NE)	1 Stage	1999	6	Extracted R-344-11-A-14; Preliminary extraction process test site	S ○ ○ ○ ● ○ ○ N
R-344-18	Vine Street near I-15 (West side)	1 Stage	1998(?)	6	Did not locate	○ ○ ○ ○ ○ ○
R-345-03	4500S and I-15 (45ft SW)	1 Stage	1998	6	Extracted R-345-3-A-16	N ○ ○ ○ ○ ○ ● S
R-345-04	4500S and I-15 (75ft NW)	1 Stage	1998	12	R-345-4-A-17; Extracted from lower set (3.7ft)	S ● ○ ○ ○ ○ ○ N
R-345-09	4500S and I-15 (SE)	1 Stage	1999	6		○ ○ ○ ○ ○ ○
R-345-10	4500S and I-15 (45ft NE)	1 Stage	1999	12	Extracted R-345-10-A-18 from lower set (2.3ft)	N ● ○ ○ ○ ○ ○ S
R-346-01C	I-15 near 500 W and 3650 S (West side; 175ft from N. end)	2 Stage	1999	18	Near USU test site; extracted R-346-1C-A-20 from lowest set (6.1ft)	N ○ ● ○ ○ ○ ○ S
R-346-05A	3300S and I-15 (SE)	1 Stage	1998	6		○ ○ ○ ○ ○ ○
R-346-08	3300S and I-15 (95ft NW)	1 Stage	1999	12	Extracted R-346-8-A-19 from lower set (4.1ft)	N ● ○ ○ ○ ○ ○ S
R-351-09	400S and I-15, along 765W (150ft SE)	2 Stage	1998	12	Extracted R-351-9-A-9 from lower set (5ft), R-351-9-B-10 from upper set (10ft)	S ○ ○ ○ ○ ○ ● N
R-351-26	N Temple and I-15 (190ft SE)	2 Stage	1998	6	Extracted R-351-26-A-13; I-15 project test wall section	S ● ○ ○ ○ ○ ○ N
R-351-30	300N and I-15, 305 N. Argyle Ct. (60ft NE)	2 Stage	1998	6	Extracted R-351-30-A-12; In backyard of residence	S ○ ○ ○ ○ ○ ● N
R-351-34	400S; West abutment of Viaduct (South side; 130ft from E. end)	2 Stage	1998	6	Extracted R-351-34-A-11	W ○ ○ ○ ○ ○ ● E
R-351-50	400S; West abutment of Viaduct (North side; 26ft from E. end)	2 Stage	1998	6	Extracted R-351-50-A-21; Extraction process demonstration site	E ● ○ ○ ○ ○ ○ W

Twenty-two coupons, representing approximately 10% of the total number of coupons were extracted as part of this current research effort. These coupons are identified in the last two columns of Table 3. The selection of coupons for extraction was largely based on accessibility, with nearly all of the coupons being within 6 feet of existing grade. Again, the cardinal directions (e.g., NW) listed in the table refer to the corner of the bridge abutment or side of the freeway nearest the coupons, while the distance from this corner or bridge end to the coupon site is noted for all sites where coupons were extracted. The last column in the table indicates graphically which coupon in the set of six was extracted as viewed when looking at the wall face. The last number of the extracted coupon identification label (e.g., the 13 in the label R-351-26-A-13) is a sequential number from 1 to 22 corresponding to the order in which the coupon was extracted.

THIS PAGE LEFT INTENTIONALLY BLANK

3.0 COLLECTION OF DATA

To realize the objectives of this project, three tasks related to data collection were undertaken. The first task consisted of collecting existing information regarding the coupon installations. The second task consisted of developing a procedure for coupon extraction, while the third task consisted of implementing the procedure in production mode and extracting the wire coupons.

3.1 Collection of Existing Information

To obtain information regarding the MSE wall reinforcement coupons, we first reviewed the information contained in UDOT's MSE wall inventory database. We next solicited Terracon and Woodward Clyde (now URS Corporation) who were the geotechnical design engineers on the I-15 Corridor Reconstruction Project for information from their project files (all of the coupons come from walls constructed as part of that project). We also contacted Mr. Si Sakhai who was UDOT's representative (now retired) on the I-15 geotechnical engineering task force, as well as several other individuals who worked on the project. Our findings were somewhat limited due to the fact that much of the project documentation was poorly organized and/or has already been purged from various storage systems. We were, however, able to locate MSE wall design requirements, project specifications (with subsequent revisions), multiple drawings, and some design calculations and memoranda from the MSE wall manufacturer VSL (later named Foster Geotechnical, now part of RECO [Reinforced Earth Company]). Unfortunately, we were unable to find precise information (e.g., coupon thicknesses and weights before and after galvanization) for the specific wire coupon installations.

A typical detail for the installation of steel wire coupons (also referred to as "inspection wires") for the I-15 Corridor Reconstruction Project is shown in Figure 3. The coupons were size W11 (MW 71) steel wire conforming to ASTM A 82. (A W11 wire has an approximate cross-sectional area of 0.11 in² (71 mm²) and nominal diameter of 3/8 or 0.374 inches (9.5 or nominally 10 mm)). These types of wires were used in fabricating the MSE walls' welded wire mesh per ASTM A 185. The wire coupons were threaded at one end and can be accessed via a 2-inch (50 mm) diameter access hole in the concrete wall panel. According to the detail, the extractable wire coupons were to be 6.56 ft (2.000 m) long.

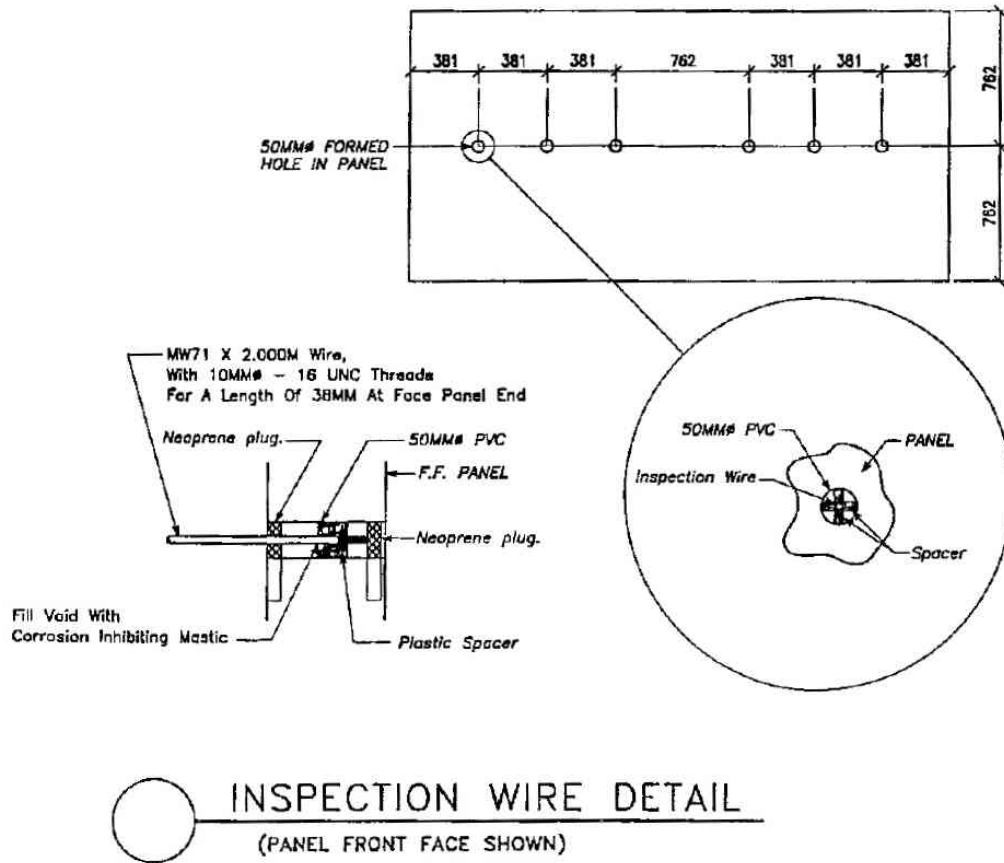


Figure 3 Typical detail for the installation of steel wire coupons for the I-15 Corridor Reconstruction Project

Project specifications and drawings indicate that the steel wires should have a minimum yield strength of 65 ksi (448 kPa). All steel wires were to be galvanized per ASTM A 123 / AASHTO M 111 which specifies a minimum thickness of 86 micron (sometimes described as 85 micron or an 85 “thickness grade,” based on a soft metric conversion) per surface. A galvanization thickness of 86 micron can alternatively be expressed as 3.4 mil, where a “mil” is one one-thousandth (i.e., 0.001) of an inch or 25.4 micron (also referred to as micrometers or μm). A galvanization thickness of 86 micron can also be expressed as approximately 610 g of zinc galvanization per square meter of surface area which is equivalent to approximately 2.0 oz/ft².

In Section 6.9.3.5.4 of UDOT’s Request for Proposals (RFP) for the I-15 Corridor Reconstruction project, several MSE wall design requirements were provided, including a

statement that “soil reinforcement for MSE and modular walls shall be steel, galvanized or epoxy coated (0.45 mm minimum coating thickness), with 28 micrometers/year sacrificial metal (based on a 75-year design life); or geogrids meeting creep requirements of AASHTO Standard Specifications for Highway Bridges.” Another requirement given in the RFP was that “the Contractor shall embed 18 retrievable samples of steel soil reinforcement in the soil mass per 150 sq. m of wall at 200 m spacing.”

Apparently, the requirements of the RFP were interpreted by project designers as meaning that “no useful life” was attributed to the galvanization and all accommodations for corrosion was incorporated into the sacrificial steel thickness. Design calculations and memoranda by the MSE wall manufacturer (for example, see memorandum regarding “2-stage MSE Wall Design and Construction Procedures” by Neely (1998)), indicate that a constant steel corrosion rate of 0.55 mil (14 micron) per surface per year [where 14 micron is the radial distance associated with a diametral distance of 28 micron] was used in the design, resulting in a total loss in wire diameter of approximately 83 mil (2.1 mm) for the 75-year design life of the MSE walls. (However, we also note that we found some calculations, which may have been preliminary, which used a corrosion rate of 15 instead of 14 micron). The FHWA/AASHTO galvanization thickness requirement of 3.4 mil (86 micron) per surface was still implemented (although its protective value was discounted), indicating that the design for corrosion for the I-15 MSE walls was conservative relative to the then-current FHWA/AASHTO procedure which would have required a sacrificial steel thickness or diameter loss of approximately 56 mil (1.4 mm) after zinc depletion. This 28 mil difference due to discounting the contribution of the zinc galvanization equates to an increase in nominal life expectancy of approximately 29 years.

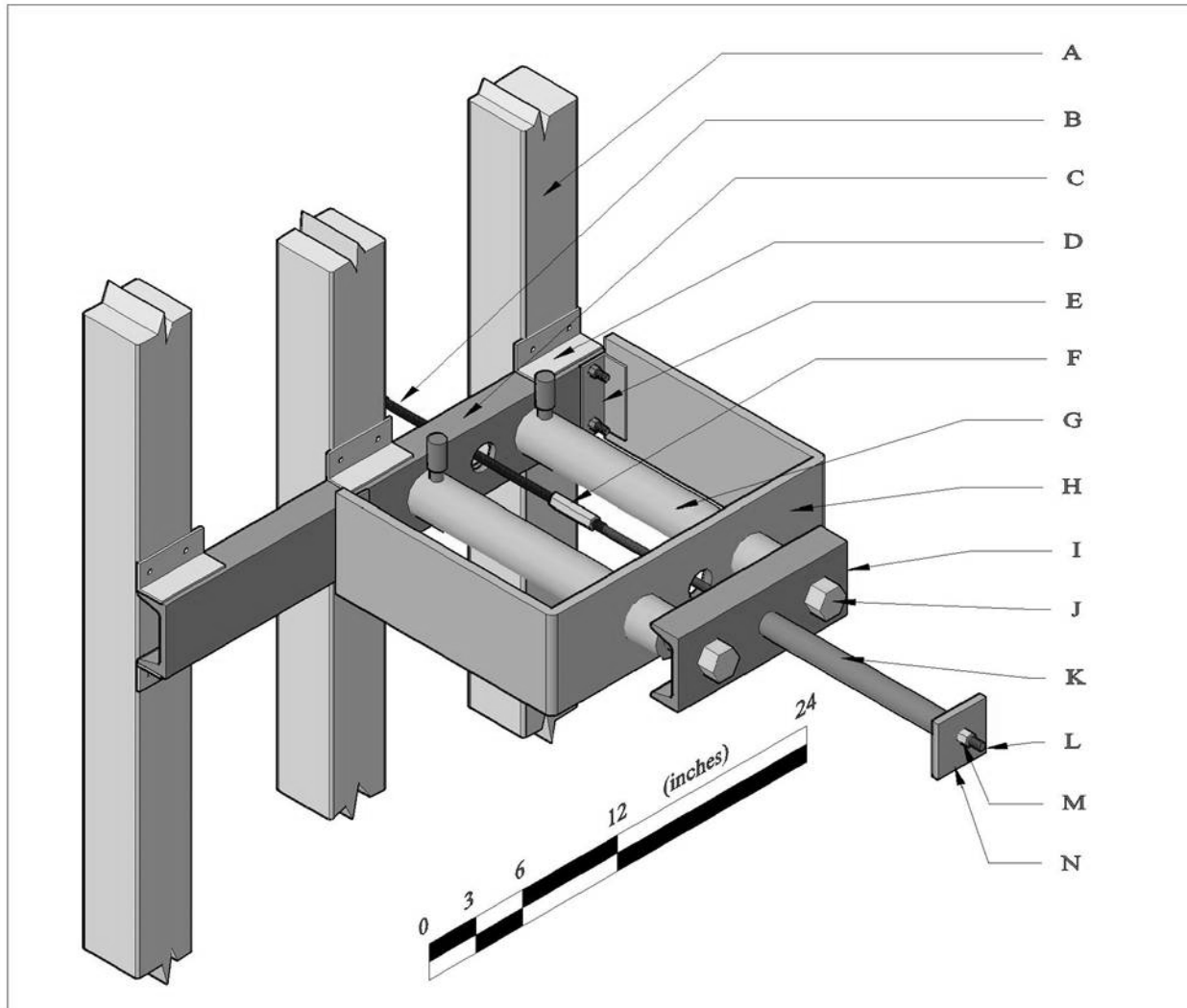
3.2 Development of Coupon Extraction Procedure

At the onset of the project, we evaluated several different methods for extracting the wire coupons from the walls. Three criteria were used in designing the extraction process. First, the extraction equipment needed to be highly portable (which would typically preclude using an electric power supply or generator) to accommodate sites where vehicle access was unavailable and/or several lanes of traffic had to be crossed quickly on-foot. Second, the extraction device would need a relatively large stroke in order to extract the nominal 79-inch (2.0-m) long coupons in a time-efficient manner. Thirdly, we were concerned that a large reaction force, locally

concentrated at the base of a jack or similar device, might damage or cause a misalignment of two-stage MSE wall panels where horizontal support from turnbuckles extending across the gap behind the panel between the first and second stages of the wall would be limited. Hence, the extraction equipment and procedure had to be designed such that the reaction load from pulling out the coupon was distributed across multiple wall panels.

One initial approach we evaluated involved using a 5-ft long, 7-kip “handy-man” type jack mounted to a lumber reaction frame. Unfortunately, the base of the jack unexpectedly cracked during our initial extraction attempt. Also, the jack tended to tip sideways as it pulled (i.e., lifted) the coupon from the hole. While not a primary objective of this research, we wanted to be able to quantify the amount of force needed to extract the coupons and this capability was not possible with the handy-man jack approach.

Ultimately we constructed an extraction device consisting of two 10-ton, 12.25-inch stroke hydraulic jacks. A schematic of the device is shown in Figure 4. The nominal 2.25-inch diameter jacks were arranged in parallel within a separable metal frame/enclosure, while a metal crosspiece was used to bridge across the ends of the two pistons, enabling the pistons to act in tandem as they were extended. A length of high strength (125 ksi) threaded rod was used to connect the reinforcement coupon through the center of the crosspiece, with a high strength coupler to attach to the coupon and a high-grade nut and flat-plate washer to attach on the other side of the crosspiece. To facilitate threading the coupler onto the coupon, a threaded die was used to remove galvanization from the threads. The two jacks were connected to a common hydraulic line, and pressure was provided by a 10,000 psi capacity hydraulic hand pump. The jacking device was mounted against the MSE wall using a wood reaction frame. Thus, the reinforcement coupons were pulled (i.e., lifted) up between the two jacks as the pistons were extended. At the end of the stroke, the pistons and crosspiece were retracted, leaving the end of the threaded rod with its nut and plate-washer now out beyond the end of the jacks. A heavy-duty 1-inch diameter pipe spacer (i.e., pipe extension) was inserted between the crosspiece and the end of the threaded rod, enabling the jacks to be used again to push/pull the coupon out further. Progressively longer pipe spacers were used as the coupon extended further out from the wall.



- | | |
|--|---|
| A. Reaction Frame (Typ. of 3), 4" x 4" Lumber | H. Jack Enclosure Frame, 5-1/2" x 3/8" Plate Steel Bent into U-shape, Drilled with (2) 2-5/16" Ø Holes for Supporting Jacks and (1) 1-1/2" Ø Center Hole for Extension Rod, Coupler, and Coupon |
| B. Wire Coupon (shown displaced/extracted from original position) | I. Crosspiece, C4x7.2 x 12", Drilled with 1" Ø Hole for Attachment Bolts, and 1-1/2" Ø Center Hole for Extension Rod, Coupler, and Coupon |
| C. Steel Base Element, C4x7.2 x 30", Drilled with (4) 5/16" Holes for Mounting Jacks and (1) 1-1/2" Ø Hole for Extension Rod, Coupler, and Coupon | J. Jack Attachment Bolt (Typ. of 2), 1-8 UNC x 1", Pre-threaded into Piston of Jack |
| D. Attachment Angle (Typ. of 6, 3 Each Side), 1-1/2" x 1-1/2" x 4", Welded to Base Element, Drilled with (2) 1/4" Ø Holes for Screws, Attachment Height on Reaction Frame Varies | K. Pipe Spacer, 1" Ø Thick Wall Pipe, Length Varies |
| E. Connection Angles (Typ. of 2), 1-1/2" x 1-1/2" x 4", Welded to Jack Enclosure Frame, Drilled for and Connected by (2) 5/16"-18 UNC x 1" Studs Welded to Base Element | L. Extension Rod, Grade 8 (min.), 3/8"-16 UNC Thread x 24" |
| F. Coupon Coupler, Grade 5, 3/8"-16 UNC x 2" | M. Nut, Grade 5 (min.), 3/8"-16 UNC |
| G. 10-ton Hydraulic Jack (Typ. of 2), Power Team Model # C1012C | N. Flat Plate Washer, 3" x 3" x 3/8" with 3/8" Ø Center Hole |

Figure 4 Schematic for extraction device

The jack assembly was attached to a load distribution frame consisting of 4x4-inch lumber using hardened-steel woodscrews. The three vertical uprights of the frame were spaced horizontally such that when the space between two uprights was centered over the end coupon of the set of six coupons, the third upright was resting on an adjacent MSE wall panel. The spacing was symmetric so that coupons at either end of the set could be accessed without rotating the frame end-to-end 180 degrees and still have load distributed beyond the single panel in which the coupon was located. Using woodscrews to mount the approximately 75-lb jack assembly to the frame in the field readily accommodated differing coupon heights above grade. The 10-ft tall, 30-inch wide frame was braced vertically against the MSE wall using one or two 2x4-inch wood kickers anchored to the ground. Figure 5 shows the general setup of the jack assembly and reaction frame for an extraction procedure. In the case of a shorter wall with overlying coping, the frame was rotated from vertical and braced into position as shown in Figure 6.



Figure 5 Setup of equipment for coupon extraction



Figure 6 Alternate setup of equipment for coupon extraction

3.3 Coupon Extraction and General Observations

During the month of June 2010, twenty-two wire coupons were extracted from select MSE walls. Fifteen coupons were from one-stage walls and seven were from two-stage walls. A detailed list of these coupons was presented previously as part of Table 3 in Section 2.5. Our field observations confirmed that all of the coupons consisted of size W11 (MW 71) steel wire with a 16-UNC threaded end. All of the wire coupons were galvanized steel, but the conditions in the access hole often varied from those shown previously in Figure 3. In no case was the void in the hole filled with “corrosion inhibiting mastic.” In most cases, the void was unfilled and the threaded end of the wire was either left exposed behind the neoprene plug or covered by a plastic cap. In a couple of instances the void was filled with an expansive aerosol foam which appeared to trap water within the hole. The actual lengths of the nominally 78.7-inch (2.000-m) long wire coupons were found to range from approximately 77.9 to 123.8 inches. Generally, the galvanization appeared to be intact but exhibited a variable amount of white oxidation product, sometimes referred to as “white rust.” A photograph showing the typical condition of the coupons is shown in Figure 7.



Figure 7 Typical condition of extracted wire coupons

In some places the galvanization appeared to have flaked or spalled from the underlying steel. A minor amount of localized steel corrosion (i.e., “red rust”) was observed on several of such specimens. Photographs illustrating these conditions are presented later in Section 4.2.3.

After extracting the coupons from the two-stage walls, we tried to observe the condition of the vertical welded wire mesh facing through the 2-inch access holes. We were generally able to see one or two segments of wire and/or portions of the loops/clevis ends for the connectors across the gap between the first and second stages of the wall. A typical view through an access hole for a two-stage MSE wall is shown in Figure 8. Generally, the conditions of these elements with respect to corrosion appeared to be similar to (or at least no worse than) those exhibited by the coupons themselves.

During the extraction process, the hydraulic pressure used to extract the coupons was recorded at select coupon displacement intervals. These pressures were subsequently related to force, thus providing a relationship between pullout resistance and displacement for the coupons. In some instances, rather than using the jacks when a coupon’s pullout resistance was small, the pipe spacer was used as a slide hammer to manually extract the coupon. The amount of manual

effort was roughly correlated with directly measured jack pressures. This correlation was developed by alternately using the jack and slide hammer techniques while extracting the full length of certain coupons.



Figure 8 Typical view of welded wire mesh through coupon access hole in two-stage MSE wall

THIS PAGE LEFT INTENTIONALLY BLANK

4.0 ANALYSIS AND INTERPRETATION OF CORROSION DATA

4.1 Methods of Analysis

As previously discussed, we were unable to find precise information regarding the reinforcement coupons (e.g., thicknesses and weights before and after galvanization) in the files of UDOT and its engineering consultants. Review of project specifications and applicable ASTM standards indicates that the manufacturing tolerance of W11 wire with respect to diameter is plus-or-minus 0.004 inch or 4 mil. Interestingly, FHWA/AASHTO design guidelines for corrosion protection and reinforcement rupture design do not seem to address or consider manufacturing tolerances, although a difference of 4 mil corresponds to a change of only about 4 years in the design life for the steel. Because of the uncertainty regarding the actual diameter of the steel wires (with the manufacturing tolerance being a significant portion a 3.4 mil zinc coating thickness), we believed it prudent to make a direct determination of this parameter when trying to quantify the amount of corrosion occurring in the MSE wall reinforcement. Since in almost all instances the galvanization on the coupons was wholly intact, emphasis was also placed on quantifying the current amount of galvanization present.

To quantify the current amount of galvanization present on the coupons and determine the thickness of the underlying steel, the coupons were subjected to a hydrochloric acid stripping procedure in general accordance with ASTM A 90. Three specimens were cut from each wire coupon. As shown in Figure 9, the first specimen (designated as “A” or “outer sample”) is a one-foot length beginning just behind the soil-wall interface (excluding the material typically located within the panel thickness and any gap between the first and second stages of the MSE wall). The second specimen (designated as “B” or “center sample”) is the next one-foot length in the backfill after specimen ‘A’. The third specimen (designated as “C” or “inner sample”) is the last two feet of the coupon located farthest from the wall face (minus the nub-end of the wire where the galvanization bulbs and the cross-section is consequently non-uniform). The coupons were partitioned in this manner so that spatial variation of corrosion with respect to distance from the wall face could be assessed. Portions of coupons in the air space between the first and second stages of the two-stage MSE walls were not tested because they visually appeared to be in better condition than immediately adjacent portions buried in the backfill. It should be noted that the thickness determined from the acid stripping test is an average thickness over the

specimen length and local minima may exist. Inasmuch as acid stripping is a destructive test, unused portions of the coupons were saved and have been returned to UDOT for its future reference. Also, pictures of each specimen prior to stripping (together with close-ups of unique corrosion or galvanization features) are contained on the disc constituting Appendix A of this report.

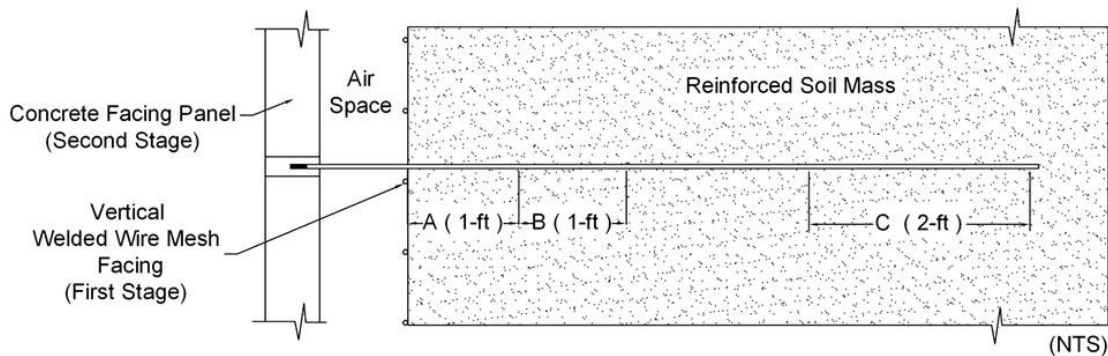


Figure 9 Segmentation of coupons into specimens for acid stripping test

To complement the data from the acid stripping test, the galvanic coatings on the specimens were measured using an electronic magnetic thickness gauge in general accordance with ASTM E 376. The reported accuracy of the DeFelsko brand “PosiTector” (series 6000 model FS1) that we used is approximately ± 2 micron (0.1 mil) plus 1% of the thickness. A set of digital calipers were also used to measure the thickness of the wire coupons both before and after the acid stripping.

To quantify the amount of corrosion in the steel, discrete micrometer measurements of the stripped steel were made in areas where the galvanization had been compromised and/or red rust was observed. These measurements were compared to the adjacent thickness measurements to determine the amount of steel lost (hence, the reported steel losses are diametral values).

4.2 Results and Discussion of Results

4.2.1 Thickness of Steel Wires

The average thickness (i.e., diameter) of specimens A, B, and C from each coupon after the acid stripping process which removes the galvanization and leaves the steel wire is shown in Table 4. In this table, coupons from one-stage walls are shown toward the top and coupons from

two-stage walls are shown toward the bottom, the two groups being separated by a horizontal line. It can be seen that the average diameter of steel wires is 0.3724 in, as compared to the nominal 0.374-inch diameter for W11 wire. However, several wires appear to have less than the minimum diameter (0.370 in) per ASTM A 82, suggesting that the sacrificial steel thickness provided may be less than that intended. However, the impact of these occurrences is mitigated by the discounting of the galvanization in resisting corrosion as was discussed in Section 3.1.

4.2.2 Thickness and Corrosion of Galvanization

The galvanization thicknesses for specimens based on the acid stripping process (“acid”) and the magnetic thickness gauge (“magnet”) are shown in terms of oz/ft² in Table 5. These thicknesses converted into units of mils (thousandths of an inch) are shown in Table 6. In these

Table 4 Steel wire thickness (diameter)

Coupon	Specimen Thickness (in)		
	"A"	"B"	"C"
R-343-7-A-6	0.3696	0.3692	0.3696
R-343-13-A-8	0.3691	0.3690	0.3698
R-343-37-A-7	0.3697	0.3696	0.3698
R-343-42-A-22	0.3708	0.3707	0.3713
R-344-1-A-3	0.3728	0.3725	0.3724
R-344-1-B-4	0.3719	0.3719	0.3724
R-344-2-A-1	0.3693	0.3696	0.3690
R-344-2-B-2	0.3712	0.3706	0.3710
R-344-4-A-5	0.3684	0.3694	0.3694
R-344-7-A-15	0.3722	0.3718	0.3727
R-344-11-A-14	0.3709	0.3707	0.3704
R-345-3-A-16	0.3693	0.3691	0.3691
R-345-4-A-17	0.3782	0.3776	0.3775
R-345-10-A-18	0.3693	0.3686	0.3693
R-346-8-A-19	0.3779	0.3782	0.3779
R-346-1C-A-20	0.3782	0.3779	0.3778
R-351-9-A-9	0.3772	0.3775	0.3785
R-351-9-B-10	0.3777	0.3778	0.3776
R-351-26-A-13	0.3711	0.3713	0.3710
R-351-30-A-12	0.3728	0.3729	0.3723
R-351-34-A-11	0.3728	0.3726	0.3725
R-351-50-A-21	0.3726	0.3719	0.3728
Average, all walls	0.3724	0.3723	0.3725
St Dev, all walls	0.0033	0.0033	0.0032
Median, all walls	0.3715	0.3715	0.3718

Table 5 Galvanization thickness (in oz/ft²) by acid stripping (“acid”) and magnetic thickness gauge (“magnet”)

Coupon	Coating Thickness Measurements (oz/ft ²)					
	Specimen A (outer)		Specimen B (center)		Specimen C (inner)	
	Acid	Magnet	Acid	Magnet	Acid	Magnet
R-343-7-A-6	2.57	3.65	2.67	3.41	3.13	3.65
R-343-13-A-8	2.82	4.06	2.22	2.82	2.66	3.00
R-343-37-A-7	2.68	3.71	2.41	3.35	2.64	3.00
R-343-42-A-22	2.88	3.35	3.13	3.35	2.66	2.71
R-344-1-A-3	2.76	3.06	2.77	3.41	2.07	2.53
R-344-1-B-4	2.83	3.30	2.76	3.30	2.44	2.59
R-344-2-A-1	3.01	3.47	3.02	3.41	3.20	3.47
R-344-2-B-2	2.93	3.30	2.93	3.41	2.36	2.59
R-344-4-A-5	2.33	2.82	2.40	2.88	2.49	3.18
R-344-7-A-15	2.53	3.35	2.55	3.24	2.37	3.30
R-344-11-A-14	2.81	3.30	2.69	3.35	2.40	2.94
R-345-3-A-16	2.72	3.30	2.83	3.35	2.88	3.35
R-345-4-A-17	3.11	4.47	3.42	3.77	3.49	4.30
R-345-10-A-18	3.00	3.71	3.17	4.00	3.40	3.77
R-346-8-A-19	3.61	4.18	3.65	3.94	3.70	4.30
R-346-1C-A-20	4.00	4.41	4.20	4.18	3.56	3.82
R-351-9-A-9	4.06	4.30	4.01	4.24	3.53	4.18
R-351-9-B-10	3.91	4.30	3.72	- - -	3.42	3.77
R-351-26-A-13	3.35	3.41	3.18	3.30	3.49	4.06
R-351-30-A-12	2.63	3.30	2.34	2.94	2.84	2.82
R-351-34-A-11	2.75	2.71	2.61	3.18	2.43	2.47
R-351-50-A-21	3.06	3.35	3.05	3.35	3.12	3.18
Average, all walls	3.02	3.58	2.99	3.44	2.92	3.32
St Dev, all walls	0.48	0.50	0.54	0.39	0.50	0.59
Median, all walls	2.86	3.38	2.88	3.35	2.86	3.24
Average, 1-stage	2.84	3.53	2.84	3.40	2.79	3.24
Median, 1-stage	2.82	3.35	2.77	3.35	2.66	3.18
Average, 2-stage	3.39	3.68	3.30	3.53	3.20	3.47
Median, 2-stage	3.35	3.41	3.18	3.32	3.42	3.77

tables, coupons from one-stage walls are shown toward the top and coupons from two-stage walls are shown toward the bottom, the two groups being separated by a horizontal line. Not shown in the tables are thicknesses based on the calculated difference in thickness as measured by the calipers before and after the acid stripping because the data is not representative. The difference-in-caliper measurements overestimate the effective amount of coating because 1) the caliper contacts measure the larger portions of the uneven micro-texture along the

Table 6 Galvanization thickness (in mils) by acid stripping (“acid”) and magnetic thickness gauge (“magnet”)

Coupon	Coating Thickness Measurements (mils)					
	Specimen A (outer)		Specimen B (center)		Specimen C (inner)	
	Acid	Magnet	Acid	Magnet	Acid	Magnet
R-343-7-A-6	4.3	6.1	4.5	5.7	5.3	6.1
R-343-13-A-8	4.8	6.8	3.7	4.8	4.5	5.1
R-343-37-A-7	4.5	6.2	4.1	5.6	4.4	5.1
R-343-42-A-22	4.9	5.6	5.3	5.6	4.5	4.6
R-344-1-A-3	4.7	5.2	4.7	5.7	3.5	4.3
R-344-1-B-4	4.8	5.6	4.7	5.6	4.1	4.4
R-344-2-A-1	5.1	5.8	5.1	5.7	5.4	5.8
R-344-2-B-2	4.9	5.6	4.9	5.7	4.0	4.4
R-344-4-A-5	3.9	4.8	4.0	4.9	4.2	5.4
R-344-7-A-15	4.3	5.6	4.3	5.5	4.0	5.6
R-344-11-A-14	4.7	5.6	4.5	5.6	4.0	5.0
R-345-3-A-16	4.6	5.6	4.8	5.6	4.9	5.6
R-345-4-A-17	5.2	7.5	5.8	6.3	5.9	7.2
R-345-10-A-18	5.1	6.2	5.3	6.7	5.7	6.3
R-346-8-A-19	6.1	7.0	6.2	6.6	6.2	7.2
R-346-1C-A-20	6.7	7.4	7.1	7.0	6.0	6.4
R-351-9-A-9	6.8	7.2	6.7	7.1	6.0	7.0
R-351-9-B-10	6.6	7.2	6.3	---	5.8	6.3
R-351-26-A-13	5.6	5.7	5.3	5.6	5.9	6.8
R-351-30-A-12	4.4	5.6	3.9	5.0	4.8	4.8
R-351-34-A-11	4.6	4.6	4.4	5.4	4.1	4.2
R-351-50-A-21	5.2	5.6	5.1	5.6	5.2	5.4
Average, all walls	5.1	6.0	5.0	5.8	4.9	5.6
St Dev, all walls	0.8	0.8	0.9	0.7	0.8	1.0
Median, all walls	4.8	5.7	4.9	5.6	4.8	5.5
Average, 1-stage	4.8	6.0	4.8	5.7	4.7	5.5
Median, 1-stage	4.8	5.6	4.7	5.6	4.5	5.4
Average, 2-stage	5.7	6.2	5.6	5.9	5.4	5.8
Median, 2-stage	5.6	5.7	5.3	5.6	5.8	6.3

galvanization’s surface and 2) the measured thickness includes zinc corrosion products (i.e., zinc oxide) which typically exhibit a bulking factor of about 1.3 based on unit weights. The significant disparity between the difference-in-caliper measurements (with average and median values of 4.89 and 5.03 oz/ft², respectively, for the 66 specimens) and those obtained using the other two methods illustrate why this method should not be used in corrosion assessments. Considering that the magnetic thickness gauge may be subject to some of the same influences as

the caliper (plus the inherent difficulties in making accurate measurements on a surface of the wire), together with guidance given in ASTM A 123 where the acid stripping method is considered the referee method in the event of conflicting measurements, we consider the galvanization thicknesses based on the acid stripping method to be the most accurate and all further assessments of corrosion in this report will be based on this data. Treating each of the 66 coupon specimens as an independent data point, the average and median galvanization thicknesses for the coupons are 2.97 oz/ft² (5.0 mil) and 2.86 oz/ft² (4.8 mil), respectively. Averaging data from specimens A, B, and C into a single data point to represent each coupon (where the averaging is weighed according to specimen length), the average and median galvanization thicknesses for the 22 coupons are a similar 2.96 oz/ft² (5.0 mil) and 2.83 oz/ft² (4.8 mil), respectively. Again, the specified amount of galvanization at installation was 2.0 oz/ft² (3.4 mil).

The thickness of the coupon galvanization based on acid stripping as shown in Table 6 is presented graphically in Figure 10. In this figure, one-stage MSE walls are grouped on the left and placed in order of decreasing age from left to right, and two-stage MSE walls are grouped on the right and again placed in order of decreasing age from left to right. It should be noted that the maximum time differential between all of the walls is less than two years (although they all are approximately eleven to twelve years old), and construction dates more precise than the year built are not available.

It can be seen from the data that in all instances the amount of galvanization currently present on the specimens exceeds the amount specified at installation (3.4 mil or 2.0 oz/ft²). Based on AASHTO's design corrosion rate, 3.4 mil of galvanization should be consumed after sixteen years or about 0.5 mil remaining after eleven years. Even after acknowledging that the AASHTO design rates are conservative, it is still surprising that after eleven to twelve years so much galvanization is present (even exceeding the initially specified amount). Unfortunately, because the initial galvanization thickness is unknown, we are unable to estimate a reliable corrosion rate prior to the present time. However, the data describing current conditions can be used as baseline information going forward to compute corrosion rates in the future.

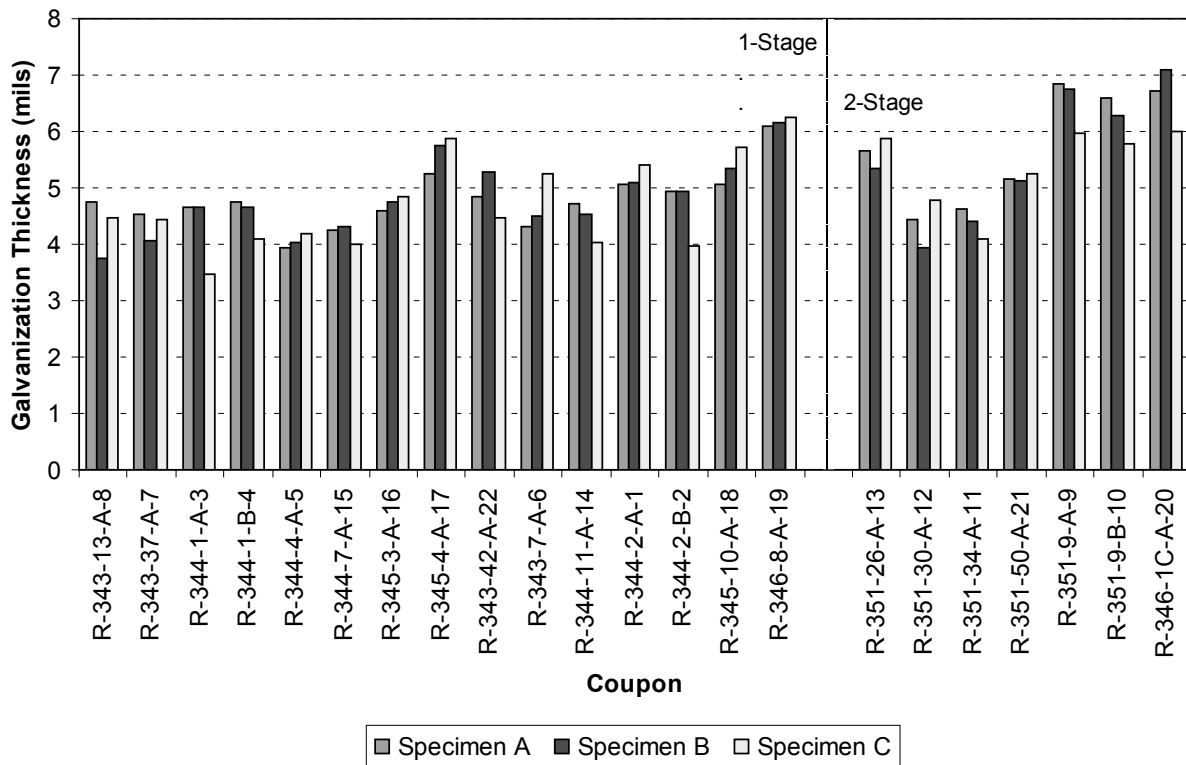


Figure 10 Variation in coupon galvanization thickness

In an attempt to roughly approximate a corrosion rate, one might utilize the apparent trend in bar height from left to right (i.e., older to younger) in Figure 10 for the two different types of MSE walls. Unfortunately, since there is only one data point in 1999 for the two-stage MSE walls, any estimated rate for two-stage walls would be tenuous at best. A linear regression with respect to year built for the one-stage MSE walls indicates a corrosion rate of about 0.55 mil/year/surface. While this rate is similar to the AASHTO design rate for galvanization for the first two years after installation, the corrosion rate at this point in the walls' design life with galvanization still present is expected to be much less (consistent with the change in design corrosion rate for zinc after two years as shown previously in Table 1), leading us to doubt the accuracy of the calculated rate. Greater reliability could be realized if the time interval over which the regression was performed were greater than the nominal one-year time frame and more data points were available. It is also possible that the elevated rate partially reflects a seasonal or longer-duration variation in metal loss, the existence of which has been recognized by previous investigators (e.g., Fishman and Withiam (in press)).

Examining the data in Figure 10 to identify other corrosion trends, taken as a group, there seems to be little appreciable or consistent difference in galvanization thickness among the specimens located at different distances back from the face of the MSE wall. There may be a slightly elevated rate away from the wall face (which is the opposite of what we would initially suspect given the greater potential access to oxygen and moisture variations near the wall face). As indicated previously in Table 6, the average thickness of the 22 innermost specimens (specimens “C”) is 4.9 mil whereas the average thickness of the 22 outermost specimens near the wall face (specimens “A”) is 5.1 mil, a difference of about 0.2 mil. Since this difference represents about 3% of the overall average of the galvanization thickness for the 22 coupons (and recognizing that the trend is not discernable when considering median values rather than average values), any spatial differences seem to be materially negligible.

When examined with respect to wall type (recognizing that there is limited data with only 15 and 7 one- and two-stage MSE walls, respectively), the spatial pattern of decreasing thickness with increasing distance away from the one-stage walls is slightly more pronounced when considering median values (which may be more representative of “typical” conditions than average values because outlying data points can have greater effect when the sample number is small). In this case, the thickness of the innermost specimens is 4.5 mil whereas the thickness of the outermost specimens is 4.8 mil, a difference of about 0.3 mil (or about 2 years of galvanic corrosion based on AASHTO design rates). For the two-stage MSE walls, spatial trend is irregular, with the average and median values suggesting differing trends. Consequently, we are left to conclude that there is no readily discernable difference in corrosion rate as a function of distance away from the wall face.

4.2.3 Corrosion of Steel

In a few instances, the galvanization had been compromised and the underlying steel showed a minor amount of red rust. In other instances, the underlying steel appeared to still be protected by the anionic behavior of the zinc. The compromised galvanization may have resulted from corrosion, but often it appeared that the galvanization may have been damaged during fabrication, construction and/or installation. The amount of steel loss in affected locations is shown in Table 7. In this table, coupons from one-stage walls are shown toward the top and coupons from two-stage walls are shown toward the bottom, the two groups being

separated by a horizontal line. To determine the amount of steel loss, a set of digital calipers were used to measure the specimen thickness at the affected location (after stripping) and this thickness was compared to adjacent thicknesses similarly measured. Locations of exposed steel were also photographed, a majority of which are shown in Figures 11 through 16. Among these pictures are the most extreme instances of corrosion and/or damage that we observed.

Table 7 Amounts of localized steel corrosion

Coupon	Specimen	Steel Loss (in)
R-343-42-A-22	A	0.0003
R-344-1-A-3	A	0.0009
R-344-1-B-4	A	0.0003
R-344-7-A-15	A	0.0006
R-344-7-A-15	B	0.0006
R-344-11-A-14	C	0.0006
R-345-4-A-17	A	0.0002
R-345-4-A-17	C	0.0004
R-346-8-A-19	C	0.0015
R-351-9-B-10	- - -	0.0010

Because of the uncertainty of the corrosion rate for the galvanization, determining a rate for the subsequent corrosion of the steel is equally problematic. The localized corrosion of coupon R-346-8-A-19 is appreciably greater than that observed in the other coupons, and future corrosion assessments should place particular emphasis on this one-stage MSE wall. There is no readily available explanation for this particularly elevated amount of localized steel loss. Only one coupon from the two-stage MSE walls (R-351-9-B-10) exhibited observable steel corrosion, and this appeared to be attributable to significant damage to the galvanization during construction and installation of the coupon.

The center portion of coupon R-344-1-A-3, specimen A, is shown in Figure 11. In the upper photograph, it appears that the zinc coating was damaged near the end of the galvanization process, leaving a long narrow strip where the galvanization detached or peeled away from the steel. Fortunately, corrosion of the underlying steel was not observed in this particular segment. However, in the lower photograph showing an area of similarly peeled zinc coating (notice the sharply defined edges for the zinc coating), steel oxidation has started. Fortunately, this corrosion is localized to only a small portion of the exposed steel, and the oxidation is shallow in

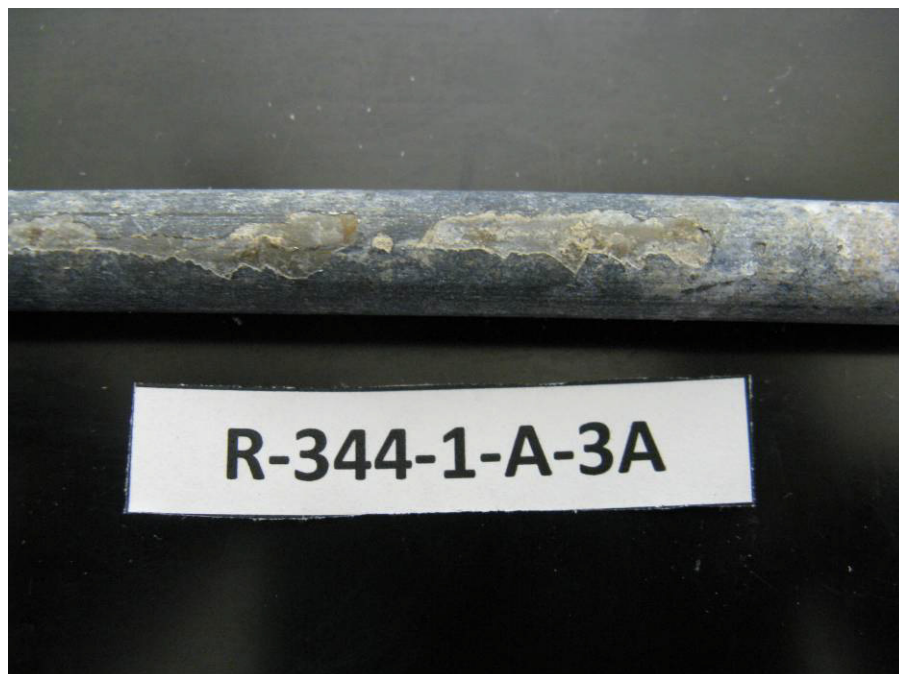
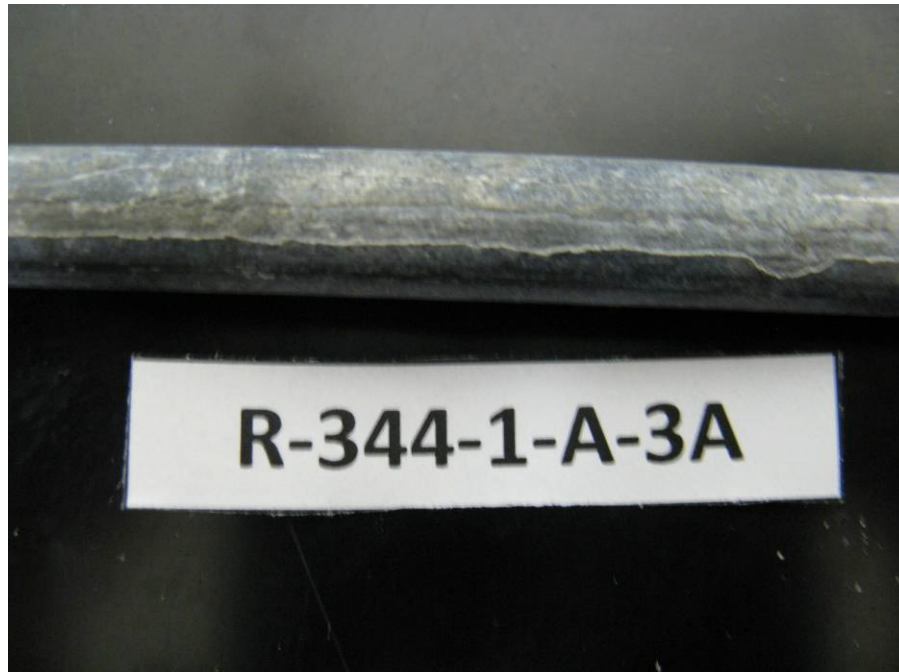


Figure 11 Photographs detailing damage/loss of galvanization for coupon R-344-1-A-3



Figure 12 Photograph detailing corrosion by localized pitting on coupon R-344-1-B-4, specimen A



Figure 13 Photograph detailing corrosion on coupon R-344-7-A-15, specimen A



Figure 14 Photograph detailing corrosion of galvanization and steel on coupon R-343-42-A-22, specimen A



Figure 15 Photograph detailing localized corrosion on coupon R-346-8-A-19, specimen C



Figure 16 Photograph detailing localized corrosion on coupon R-345-4-A-17, specimen A

nature and absent of pitting. The presence of this kind of galvanization damage (particularly on monitoring coupons rather than production reinforcement) suggests a need for more effective inspection of MSE wall materials prior to installation.

Figure 12 shows a section of coupon R-344-1-B-4, specimen A, located immediately behind the inner neoprene plug in the access hole. This section exhibits several small locations of steel oxidation (i.e., red rust). Figure 13 shows similar, but somewhat larger, areas of steel corrosion on coupon R-344-7-A-15, specimen A. A small area of the galvanization is missing, and the exposed steel is showing some oxidation with a textured surface beginning to become apparent.

Figure 14 and Figure 15 show areas of localized steel corrosion on coupons 343-42-A-22, specimen A, and R-346-8-A-19, specimen C, respectively. The galvanization in these instances (particularly the former) appears to have smoother edges, leading us to suspect that these instances represent anionic depletion of the zinc rather than mechanical damage prior to the

corrosion of the steel. The latter instance is the greatest loss of steel that we measured. Figure 16 shows coupon R-345-4-A-17, specimen A, with an instance where steel oxidation is present on a segment of the coupon, and extends a significant portion along the coupon circumference. The measurement of diametral steel loss was taken at the darkest and apparently most severe location at the top of the specimen as shown in the photograph.

Coupon R-351-9-B-10 is of particular note with respect to the corrosion we observed. This coupon was initially extracted to help assess vertical variations in corrosion by comparing it with coupon R-351-9-A-9 which was located at the same horizontal location in a wall, but at a lower elevation. However, as the coupon was extracted, it was obvious that the coupon had been damaged either at, or prior to, installation. The bent coupon is shown in Figure 17. The galvanization appears to have flaked or spalled in the areas of greatest bending, and steel has subsequently corroded. This portion of the wire coupon was located near the wall face, just inside the panel access hole and in the open-air gap between the first and second stages of the MSE wall. Photographs showing greater detail of the damaged portions of the wire coupon are provided in Figure 18. The penetration of the rust is relatively shallow with some surface texture becoming apparent. The thickness of the flaking galvanization shown in the pictures is about 3 mil and the corrosion of the steel corresponds to a diametral loss of about 1 mil. The damage and corrosion observed on this coupon highlights the importance of avoiding excessive bending of MSE wall reinforcement elements during pre-installation handling and construction.



Figure 17 Damage and subsequent corrosion of coupon R-351-9-B-10 near panel face of two-stage MSE wall



Figure 18 Photographs detailing damage and subsequent corrosion near end of coupon R-351-9-B-10

THIS PAGE LEFT INTENTIONALLY BLANK

5.0 ANALYSIS AND INTERPRETATION OF PULLOUT RESISTANCE DATA

5.1 Methods of Analysis

While not the primary focus of this project, we measured the amount of force developed by the hydraulic jacks while extracting the coupons. In a couple of instances, we broke the threaded end of the coupons before we were ultimately able to successfully reconnect and extract the coupons. This was unexpected since preliminary calculations using estimated frictional shear strength resistance proportional to effective stress at the elevation of the coupon did not indicate such large resistances. On the other hand, in a couple of instances (coupons R-344-2-A-1, R-346-01C, and R-351-50-A-21), the reinforcement coupon spun around in place when tightening the treaded coupler, and the coupon was extracted easily. At nine of the 22 coupon installations, we pulled out the coupons by hand using a pipe spacer as a slide hammer acting against the flat-plate washer and nut at the end of the threaded connection rod. We developed an approximate correlation between the manual pullout resistance and the static pullout force measurements from the jacks. This was accomplished by alternating use of the jack and slide hammer techniques while extracting the full length of certain coupons.

5.2 Results and Discussion of Results

Table 8 presents the pullout related parameters for the reinforcement coupons. In this table, coupons from one-stage walls are shown toward the top and coupons from two-stage walls are shown toward the bottom, the two groups being separated by a horizontal line. In the pullout data, the large pullout force for coupons R-344-1-A-3, R-344-1-B-4, and R-344-2-B-2 (all from one-stage MSE walls) should be somewhat discounted because we observed that these coupons were misaligned relative to the access hole and thus noticeably rubbed against the backside of the panel as they were extracted, artificially increasing the pullout resistance. Another potential factor contributing to the pullout resistance was friction within the neoprene plug in the back of the access hole in the one-stage MSE wall panels. Staging mock pullout tests in the lab using several recovered plugs and coupons, we estimate that the contribution of the plugs to the measured pullout resistance was in the range of 20 to 70 lbs. In the case of two-stage walls, the plug in the back of the panel was either displaced (and thus not contributing to the pullout resistance) or not present.

Table 8 Parameters relating to coupon pullout resistance

Coupon	Distance (ft)		Length (ft)		Pullout Force (lbs)
	Above Ground	Below Top of Wall	Overall	Embedded	
R-343-7-A-6	5.50	35.00	6.52	6.02	2800
R-343-13-A-8	2.75	11.58	6.51	6.01	5380
R-343-37-A-7	2.08	12.42	6.51	6.43	6450
R-343-42-A-22	5.00	9.50	10.01	9.57	2150
R-344-1-A-3	3.50	7.25	10.31	9.83	7100
R-344-1-B-4	1.75	6.67	10.20	9.70	6450
R-344-2-A-1	6.00	9.42	6.52	6.08	430
R-344-2-B-2	5.25	13.17	10.06	9.60	5380
R-344-4-A-5	5.08	15.17	6.50	6.00	2040
R-344-7-A-15	3.67	6.67	10.32	9.82	2150
R-344-11-A-14	3.17	8.50	9.93	9.45	4090
R-345-3-A-16	5.75	7.50	6.52	6.13	500*
R-345-4-A-17	3.67	11.92	7.99	7.61	1500*
R-345-10-A-18	2.25	17.33	6.52	6.29	1000*
R-346-8-A-19	4.08	11.00	7.88	7.38	4620
R-346-1C-A-20	6.08	19.50	8.00	6.13	650*
R-351-9-A-9	5.00	13.50	7.99	6.41	500*
R-351-9-B-10	10.00	8.50	8.01	6.28	500*
R-351-26-A-13	5.58	18.00	10.03	8.36	1500*
R-351-30-A-12	6.75	13.08	10.00	8.58	650*
R-351-34-A-11	8.50	8.67	10.11	8.47	500*
R-351-50-A-21	6.67	13.75	10.30	8.78	540

* denotes pullout force has been approximated for manual extraction

In an effort to facilitate comparisons between coupons, the coupon pullout force can be normalized in two ways. First, the pullout force can be divided by the embedded length. Second, the pullout force can be divided by the embedded length as well as by the height of the wall above the coupon (i.e., the distance from the coupon to the top of the wall or the “overburden height”) which is a proxy for effective vertical stress. These normalized resistances are shown in Figure 19 and Figure 20. In these figures, one-stage MSE walls are grouped on the left and placed in order of increasing overburden height from left to right, and two-stage MSE walls are grouped on the right and again placed in order of increasing overburden height from left to right. In the graphs, the shading of bars has been removed for coupons which the pullout resistance is suspected to be artificially high due to friction against the edge of the access hole.

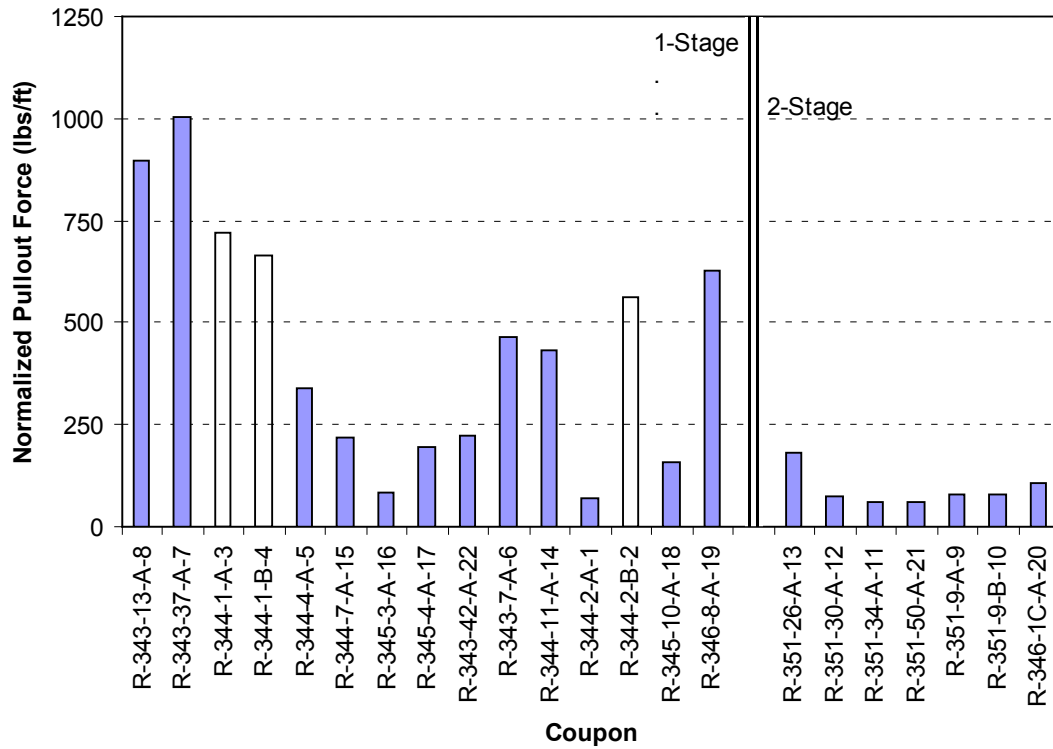


Figure 19 Coupon pullout resistance normalized by embedded length

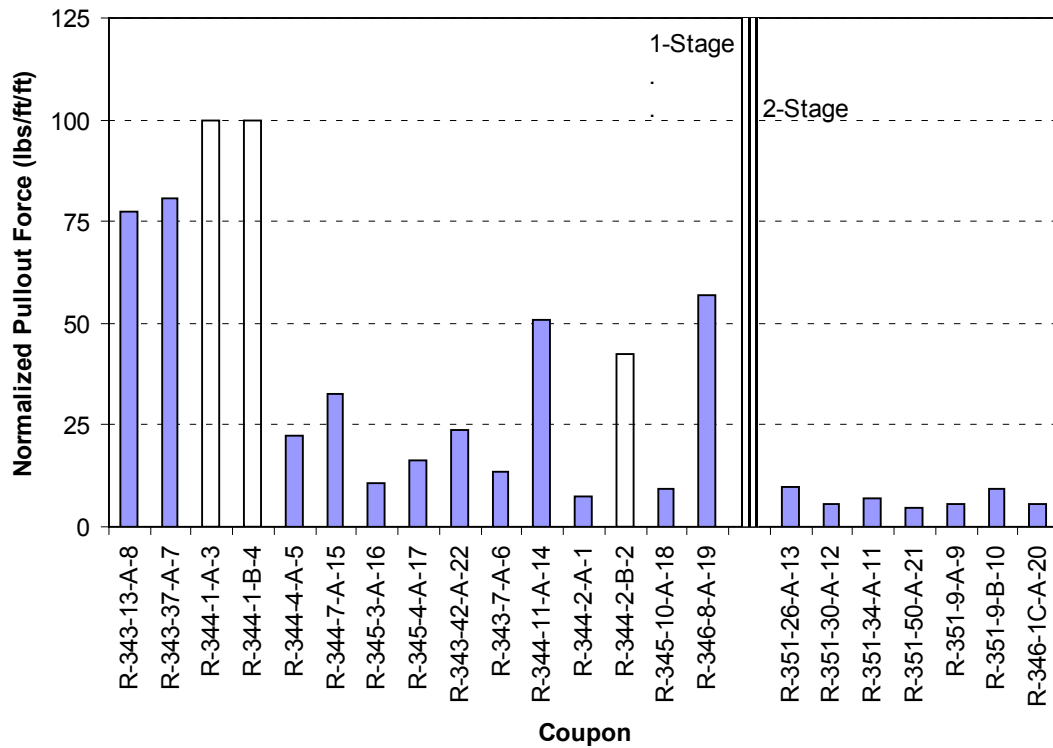


Figure 20 Coupon pullout resistance normalized by embedded length and overburden height

In these figures, it is readily apparent that peak pullout resistance for the coupons is typically much larger for one-stage MSE walls than for two-stage MSE walls. After discounting those coupons which appeared to rub on the back/side of the access hole during extraction, the average and median peak pullout resistance normalized by embedded coupon length and overburden height for the one-stage walls is about 34 and 23 lb/ft/ft, respectively; for two-stage walls, the average and median values are about 7 and 6 lb/ft/ft, respectively (a difference of about four to five times between the two wall types). We suspect that the difference in peak pullout resistance between the two types of MSE wall is attributable to an inherently lower degree of compaction near the face of the two-stage walls. Because the welded wire mesh facing is flexible relative to the standard concrete panel, it is difficult to apply a large amount of compactive energy near the wall face. In fact, many early MSE wall specifications specifically excluded compaction testing within a meter or so of the wall face because of this difficulty. In addition to affecting the compacted density of the soil near the wall face, the flexibility of the wall facing also provides less constraint on the failure surface, thus lessening the amount of shear resistance that develops prior to pullout.

Plots showing the pullout resistance of coupons at displacement intervals of approximately 3 or 6 in are presented in Figure 21. The end of the first displacement interval is shown in the figures by a hollow diamond, and the portion of the curve to the left of it might have been steeper than that shown (i.e., the peak resistance may have decreased more rapidly) had jack pressures been recorded at smaller displacement intervals. From the plots, one can see a pronounced decrease in resistance once the coupons start to move and are pulled out of the wall. While completion of the extraction process by hand prevented minimum values from being reached (values which should trend to zero as the full length of the coupon exits the wall), the pullout resistances appeared to typically approach some type of ultimate or “residual” value after several inches of displacement. The residual values ranged from about 10 to nearly 100% of the measured peak force. (The nearly 100% values correspond to coupons R-344-2-A-1 and R-351-50-A-21 which spun around in-place when trying to attach an extraction coupler).

Unfortunately, it is not possible to directly correlate the coupon pullout forces with those indicated by typical MSE wall design equations because the design equations are based on the spacing and size of the transverse wires in the welded wire mesh (for equations, see Section 3.3.b

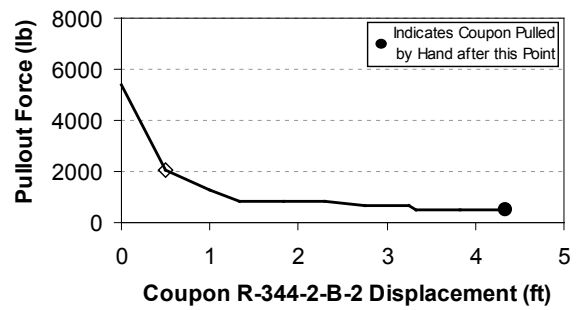
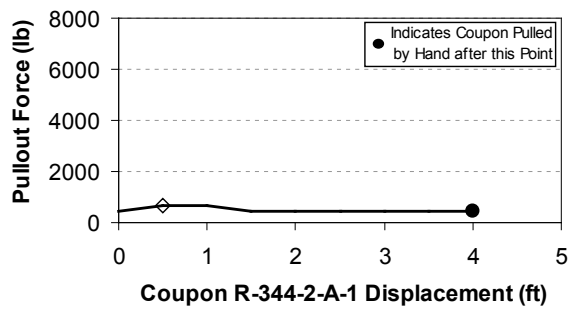
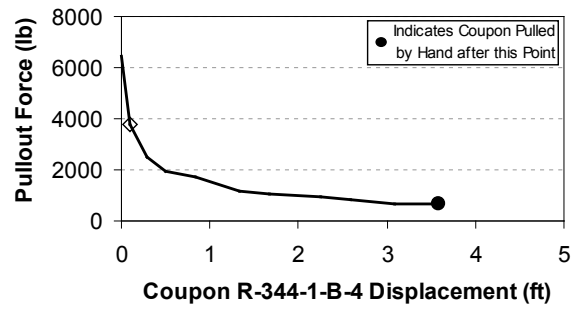
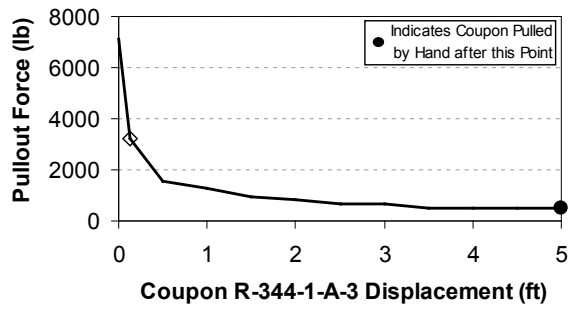
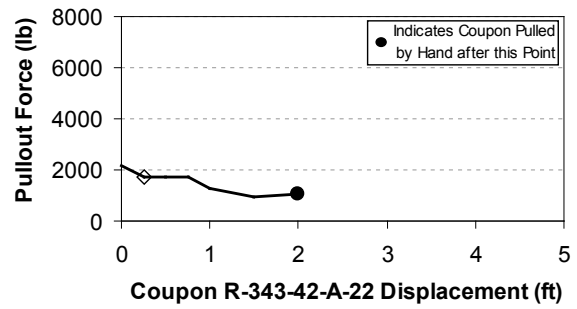
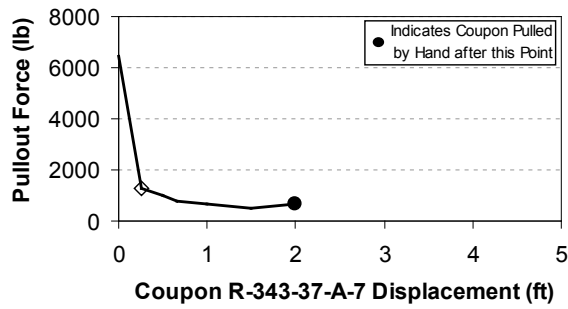
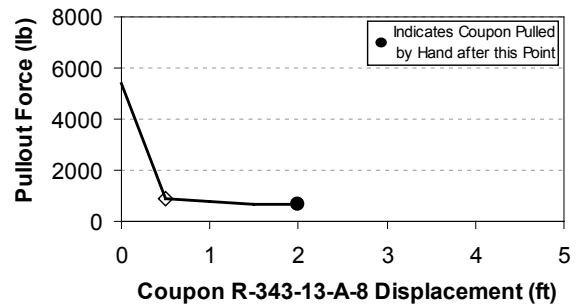
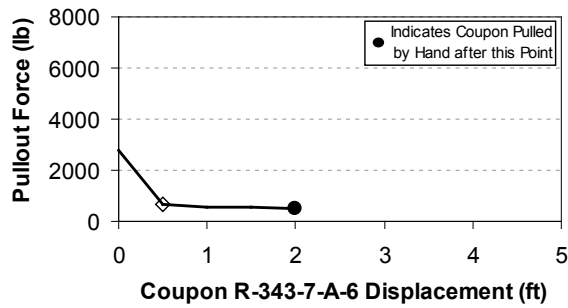


Figure 21 Coupon pullout resistance versus displacement
(continued on next page)

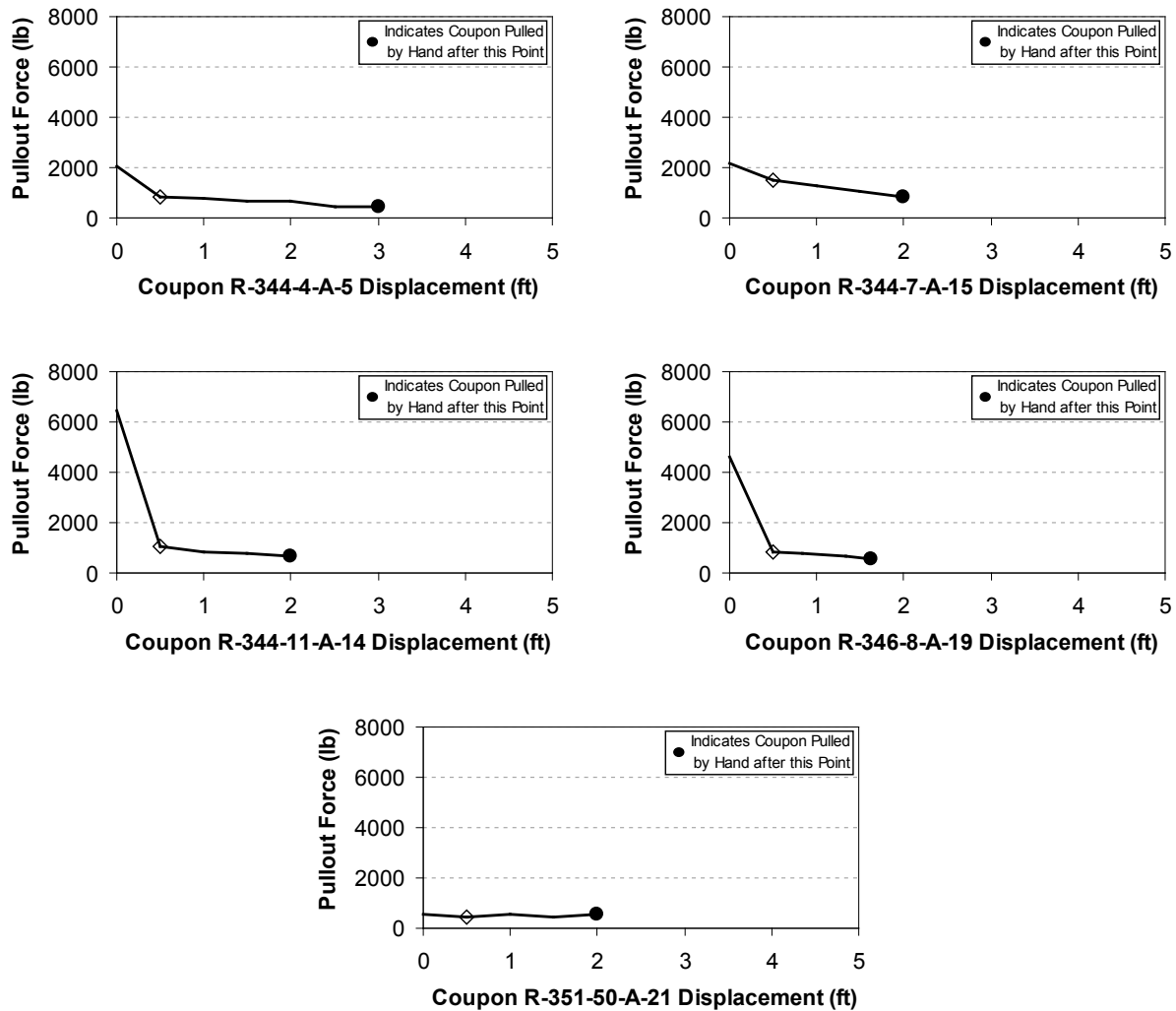


Figure 21 Coupon pullout resistance versus displacement
(continued from previous page)

of “Mechanically Stabilized Earth Walls and Reinforced Soil Slopes, Design and Construction Guidelines” by Elias et al. (2001)) and there are not any such wires on the singularly longitudinal coupons. Even if the transverse wire dimensions were not an issue, the design equations would likely not correspond to the measured pullout forces because default design parameters are based on a lower bound envelope (not a best estimate) of pullout resistance based on a number of tests / case histories (for a comparison of design and actual resistances, see Figure B-109 of “Reinforcement of Earth Slopes and Embankments” by Mitchell and Villet (1987)). However, one can perform a simplified analysis assuming a frictional slip surface around the circumference of the wire coupon. Using an interface friction angle of approximately 17 degrees (which

corresponds to a soil friction angle of 34 degrees and a soil-to-steel interface ratio of 0.5) and a unit weight for the overburden soil equal to 135 pcf, the resulting pullout force would be approximately 4 lbs per foot length per foot of overburden. This value is substantially less than the peak pullout values for the one-stage walls and much closer to “residual” values (average and median values of 7 and 8 lbs/ft/ft, respectively). This value is also similar to pullout resistances for the two-stage walls (average and median values of 7 and 6 lb/ft/ft, respectively, for peak based on seven coupons, and an average value of 4.5 lb/ft/ft for residual based on one coupon). This simple analysis may seem to suggest that 1) in the case of two-stage MSE walls, the observed pullout resistance of embedded reinforcement should be adequate with respect to theoretically-based design criteria, and 2) in the case of one-stage MSE walls, the observed pullout resistance of embedded reinforcement should be quite conservative. However, as was explained previously, these observed resistances cannot be directly compared to standard design values. Also, when assessing variability in resistance per wall type, one must consider the relative scale of the axis used in Figure 19 and Figure 20, which may make the resistances of the two-stage MSE walls appear to be more uniform. Given the dramatic difference in peak pullout resistance between the two MSE wall types, and recognizing that current MSE wall design procedures do not make a distinction in pullout resistance between one- and two-stage MSE walls, we believe it prudent to investigate this issue more thoroughly and help assure that standard one-stage wall design procedures are wholly applicable to two-stage walls.

One concern at the onset of this project was a potential risk of damaging or dislocating the facing panels in the two-stage MSE wall system when extracting the coupons. Because of the relatively low pullout resistance exhibited by these coupons, the reaction force from the jack acting on the panel was quite small and thus required less load transfer to adjacent panels than was provided by the reaction frame used. In fact, in many cases a jack was not even used to extract the coupon, but rather a manually operated slide hammer was employed, thus not transferring any load to the panel.

THIS PAGE LEFT INTENTIONALLY BLANK

6.0 CONCLUSIONS AND RECOMMENDATIONS

Based on the results of the work presented herein, the following conclusions are made and recommendations presented:

1. Twenty-two wire coupons were extracted from MSE walls that are approximately 11 to 12 years old, and the initial condition of these coupons at the time of their installation is undocumented and unknown.
2. For the MSE walls constructed as part of the I-15 Corridor Reconstruction project through downtown Salt Lake City, designers apparently attributed “no useful life” to the galvanization and all accommodations for corrosion was incorporated into the sacrificial steel thickness. This indicates that the design for corrosion resistance is quite conservative for these walls and, consequently, the probability of corrosion-related failure should be lower than normal.
3. Based on field observations, the galvanization on the coupons appeared to be intact but exhibited a variable amount of white oxidation product. In some places the galvanization appeared to have flaked or spalled from the underlying steel. A minor amount of localized steel corrosion was observed on several of such specimens. There was no readily observable evidence of excessive corrosion of the vertical welded wire mesh facing of the two-stage MSE walls.
4. Based on laboratory measurements, the average thickness of the galvanization on all of the extracted coupons currently exceeds the minimum value specified for the time of installation.
5. Because initial conditions are unknown, a reliable corrosion rate cannot be determined using the direct measurement methods employed in this study. However, the data collected regarding current conditions can be used as baseline information going forward to compute corrosion rates in the future.
6. Now that the physical conditions of the coupons are known, consideration should be given to supplementing existing data with linear polarization resistance (LPR)

measurements, a non-destructive, indirect method of determining instantaneous corrosion rates. Repeated measurements will help establish a longer term corrosion rate.

7. Several coupons appeared to have been damaged prior to, or during, installation. Also, the most significant areas of corrosion appeared to be associated with damaged galvanization. Both of these occurrences suggest the need for, and importance of, effective inspection of MSE wall materials prior to, and during, installation.
8. There is presently no readily discernable difference in corrosion conditions as a function of distance away from the wall face.
9. There was significant difference in the coupon pullout resistance between one-stage and two-stage MSE walls (with the former being about 4 to 5 times the latter). Current MSE wall design procedures do not suggest that there should be such a difference. The reasons for this behavior and their implications for design and performance should be further investigated.

REFERENCES

- AASHTO [American Association of State Highway and Transportation Officials]. (1996). "Standard Specifications for Highway Bridges." Sixteenth Edition. AASHTO, Washington, D.C.
- AASHTO [American Association of State Highway and Transportation Officials]. (2007). "AASHTO LRFD Bridge Design Specifications." Customary U.S. Units, Fourth Edition. AASHTO, Washington, D.C.
- Bay, J.A., Anderson, L., Gerber, T.M., and Maw, R.B. (2010). "An Inspection, Assessment, and Database of UDOT MSE Walls." Report to Utah Department of Transportation Research Division, Utah State University, Department of Civil and Environmental Engineering. April.
- Beavers, J.A. and Durr, C.L. (1998). "Corrosion of Steel Piling in Nonmarine Applications." NCHRP Report 408. Transportation Research Board, National Academy Press, Washington, D.C.
- Darbin, M., Jailloux, J.M., and Montuelle, J. (1988). "Durability of Reinforced Earth Structures: the Results of a Long-Term Study Conducted on Galvanized Steel," Institution of Civil Engineers, Proceedings, Part 1, Design and Construction, Vol. 84, 1029-1057.
- Elias, V. (1990). "Durability/Corrosion of Soil Reinforced Structures." FHWA-RD-89-186, Report to the Federal Highway Administration, Office of Engineering and Highway Operations, R&D, McLean, VA, by Earth Engineering & Sciences, Baltimore, MD. December.
- Elias, V. (2000). "Corrosion/Degradation of Soil Reinforcements for Mechanically Stabilized Earth Walls and Reinforced Soil Slopes." FHWA NHI-00-044. Report to the National Highway Institute, Federal Highway Administration, Washington, DC, by Ryan R. Berg & Associates, Woodbury, MN. September.
- Elias, V. and Christopher, B.R. (1996). "Mechanically Stabilized Earth Walls and Reinforced Soil Slopes, Design and Construction Guidelines. FHWA-SA-96-071. Report to the

- Federal Highway Administration, Washington, DC, by Earth Engineering and Sciences, Baltimore, MD. October.
- Elias, V., Christopher, B., and Berg, R. (2001). "Mechanically Stabilized Earth Walls and Reinforced Soil Slopes, Design and Construction Guidelines." FHWA NHI-00-043. Report to the National Highway Institute, Federal Highway Administration, Washington, DC, by Ryan R. Berg & Associates, Woodbury, MN. March.
- Elias, V., Fishman, K.L., Christopher, B.R., and Berg, R.R. (2009). "Corrosion/Degradation of Soil Reinforcements for Mechanically Stabilized Earth Walls and Reinforced Soil Slopes." FHWA NHI-09-087. Report to the National Highway Institute, Federal Highway Administration, Washington, DC, by Ryan R. Berg & Associates, Woodbury, MN. November.
- Fishman, K.L. and Withiam, J.L. (in press). "LRFD Metal Loss and Service- Life Strength Reduction Factors for Metal Reinforced Systems in Geotechnical Applications., National Cooperative Highway Research Program [NCHRP] Project 24-28 Final Report, National Academy of Sciences, Washington, D.C.
- Gerber, T.M., Bay, J.A., and Maw, R.B. (2008). "Inspection and Observed Performance of Mechanically Stabilized Earth (MSE) Walls." 41st Symposium on Engineering Geology and Geotechnical Engineering. Boise, Idaho.
- Gladstone, R.A., Anderson, P.L., Fishman, K.L., and Withiam, J. L. (2006). "Durability of Galvanized Soil Reinforcement, More than 30 Years of Experience with Mechanically Stabilized Earth." Transportation Research Record: Journal of the Transportation Research Board, No. 1975, Washington, D.C., 49-59.
- Infinitech Surface Finishing (2005). "Zinc Plating – The Corrosion-Prevention Workhorse." <<http://www.infinitechfinishing.com/Articles/Article7.htm>> (July 15, 2010).
- Jackura, K.A., Garofalo, G.A., and Beddard, D. (1987). "Investigation of Corrosion at 14 Mechanically Stabilized Embankment Sites." Publication CA/TL-87/12. California Department of Transportation.

- Mitchell, J.K. and Villet, W.C.B. (1987). "Reinforcement of Earth Slopes and Embankments." National Cooperative Highway Research Program [NCHRP] Report 290. Transportation Research Board, National Research Council, Washington D.C. June.
- Neely, W. (1998). "2-Stage MSE Wall Design and Construction Procedures." Memorandum dated October 21, 1998, to Andy Hoff of Wasatch Constructors from William Neely of Foster Geotechnical.
- Rehm, G. (1980). The Service Life of Reinforced Earth Structures from a Corrosion Technology Standpoint. Reinforced Earth Company, Vienna, VA. (unpublished).
- Romanoff, M. (1957). Underground Corrosion, National Bureau of Standards, Circular 579, U.S. Department of Commerce, Washington D.C.

THIS PAGE LEFT INTENTIONALLY BLANK

APPENDIX A

Photographs of extracted coupon specimens are contained on the accompanying disc which constitutes this Appendix.

Coupons are identified by unique labels such as R-344-1-B-4-C, where “R-344-1” corresponds to UDOT’s wall identification number and the next letter (“B”) is a sequential series corresponding to the first, second, etc., coupon extracted from that particular wall (in the case, this wire is the second coupon (“B” being the second letter of the alphabet) extracted from wall R-344-1). The next number (in this example “4”) is a sequential number corresponding to the order in which the wire was extracted (in this case the fourth wire coupon extracted) during this project. The last letter corresponds to the location of the specimen relative to the coupon’s entire length. Specifically, the letter “A” corresponds to the one-foot length beginning just behind the soil-wall interface (excluding the material typically located within the panel thickness and any gap between the first and second stages of the MSE wall); the letter “B” corresponds to the next one-foot length in the backfill after specimen “A”; and the letter “C” corresponds to the last two feet of the coupon, being located farthest from the wall face. This segmentation scheme is shown graphically in Figure 9 on the report. Because of its length, photographs of specimen C were taken in two parts – left (“L”) and right (“R”).

Physical specimens are also identifiable by numbers and letters stamped into the ends of the wire. For example, specimen R-344-1-B-4-C would be uniquely identified by the stamps “4” and “C”, where the end with the number stamp is located nearer to the MSE wall face.

THIS PAGE LEFT INTENTIONALLY BLANK